3D printing of edible hydrogels containing thiamine and their comparison to cast gels

Kamlow, Michael-Alex; Vadodaria, Saumil; Gholamipour-shirazi, Azarmidokht; Spyropoulos, Fotis; Mills, Tom

DOI:
10.1016/j.foodhyd.2020.106550

Document Version
Peer reviewed version

Citation for published version (Harvard):
Kamlow, M-A, Vadodaria, S, Gholamipour-shirazi, A, Spyropoulos, F & Mills, T 2021, '3D printing of edible hydrogels containing thiamine and their comparison to cast gels', *Food Hydrocolloids*, vol. 116, 106550. https://doi.org/10.1016/j.foodhyd.2020.106550

3D printing of edible hydrogels containing thiamine and their comparison to cast gels

Michael-Alex Kamlow, Saumil Vadodaria, Azarmidokht Gholamipour-Shirazi, Fotis Spyropoulos, Tom Mills

School of Chemical Engineering, University of Birmingham, Edgbaston, Birmingham, B15 2TT, United Kingdom

Abstract

In this study, 3% w/v kappa-carrageenan (κC) and 2% w/v agar were assessed for their suitability for hot extrusion 3D printing (3DP) and compared to cast gels of equivalent composition. Moreover, incorporation of a model active (thiamine) at varying concentrations, was studied for both 3DP and cast microstructures. Rheology and differential scanning calorimetry showed that thiamine (via electrostatic complexation) reinforced the kappa-carrageenan gel network (up to a certain threshold concentration), whereas the agar gel was structurally unaltered by the active's presence. While the κC-thiamine formulations were printable (within a relatively narrow formulation/processing window), the agar-thiamine systems were not printable via the current set up. Texture profile analysis (TPA) showed that 3DP κC-thiamine cylinders had a hardness value of 860 g ± 11% compared to 1650 g ± 6% for cast cylinders. When compressed they delaminated due to failure between consecutive layers of material deposited during the printing process; light microscopy revealed distinct layering across the printed gel structure. Release tests at 20°C showed printed gels expelled 64% ± 2.2% of the total active compared to 59% ± 0.8% from the cast gels over six hours. At 37°C these values increased to 78% ± 2.6% and 66% ± 3.5% respectively. This difference was believed to be due to the significant swelling exhibited by the printed systems. A simple empirical model, applied to the release data, revealed that thiamine discharge from 3DP gels was solely driven by diffusion while ejection of the active from cast systems had both diffusional and relaxation contributions.

1. Introduction

Additive manufacturing, also known as 3D-printing (3DP), is a layer-by-layer production method that uses digital files to create parts and products. While many different areas of industry have adopted it, its uptake as a means of manufacture at the point of production has still not caught up in areas like homes, health care facilities and pharmacies. However, despite this it is still a growth industry worth billions of dollars per year (McCue, 2012). Most research and utilisation has been focused on plastic polymers (Rahim, Abdullah, & Md Akil, 2019), metal (Buchanan & Gardner, 2019), and ceramics (Chen, et al., 2019) with the emphasis being on the small scale production of highly customised items. Other areas of interest have included pharmaceuticals (A. Goyanes, et al., 2017), biotechnology (D. Singh, Singh, & Han, 2016) and prosthesis development (Koprnický, Najman, & Šafka, 2017). The plug and play nature of 3D printing is appealing because laymen are able to connect a printer, load in the printing material and then download one of many designs from the internet, modify it if they choose to and then print it. This allows customisation at the point of demand and modification without the need for additional tooling or moulding.

From the start of the last decade, food 3DP has started to rapidly develop as an area of research. This is due to various factors such as design of complex geometries without

moulds, production of softer foods that mimic the appearance of normal foods for people with conditions such as dysphagia, while reducing production time and skill level of the person producing it as well as increasing repeatability (Kouzani, et al., 2017), and using 3D printing to precisely control ingredient placement and distribution (Diaz, Van Bommel, Noort, Henket, & Briër, 2018). However, development and subsequent uptake of food 3DP in homes and by industry has been inhibited by various issues. The major problem is that 3D printing is still too slow, with larger objects taking upwards of an hour to produce (Lin, 2015). Moreover, food systems are multifaceted, often consisting of several materials in varying ratios, sensory characteristics related to internal microstructure and thermal transition temperature as well as most food materials not being readily extrudable. This is why a lot of research into food 3DP has focused on natively extrudable food such as chocolate (Lanaro, Desselle, & Woodruff, 2019), cheese (Le Tohic, et al., 2018) and dough (Fan Yang, Zhang, Prakash, & Liu, 2018). Some non-natively extrudable food materials tested for 3D printing include fish surimi gel (Wang, Zhang, Bhandari, & Yang, 2018) and fruit (C. Severini, Derossi, Ricci, Caporizzi, & Fiore, 2018). However, most research has been directed into finding a wider range of materials that can be utilised in food 3DP as well as trying to establish an understanding of how their various properties affect their printability.

Hydrocolloid gels (hereafter referred to as hydrogels) are an area of interest in food 3DP with a large body of work directed into investigations regarding their suitability and utility in this field (Kim, et al., 2018; Z. Liu, Zhang, & Yang, 2018; Rutz, Hyland, Jakus, Burghardt, & Shah, 2015). They are considered ideal owing to the fact that many of them are renewable, widely used already in foods and pharmaceuticals and are known to be biocompatible. Hydrogel printing normally involves the cold extrusion of systems that have already set, requiring little, if any, temperature control. Cold extrusion approaches to date have included mixed hydrogels (Kim, Bae, & Park, 2017), single hydrogels (Gholamipour-Shirazi, Norton, & Mills, 2019) and the use of hydrogels as an adjunctive material (Kim, et al., 2019). The second method is the hot extrusion of hydrogels in the sol state, with the sol-gel transition occurring on the printing bed rapidly after being deposited. This has the advantage of being able to print highly viscous gels far more readily, as they would still be in the sol state unlike the gelled samples; this has been highlighted for cold extrusion (Azam, Zhang, Bhandari, & Yang, 2018) which essentially is printing yield stress materials. There exist fewer examples of hot extrusion hydrogel printing such as kappa-carrageenan (κC) with gelatin (Warner, Norton, & Mills, 2019), κC by itself (Diañez, et al., 2019) and agar with gelatin (Serizawa, et al., 2014). Another type of 3DP is freeform reversible embedding of suspended hydrogels (FRESH) which involves directly printing the hydrogel into a support bath of a second hydrogel (Hinton, et al., 2015). This allows for a range of intricate structures to be produced that more accurately mimic a cast gel. This process can also be modified to include different support bath materials such as gellan fluid gels (Compaan, Song, & Huang, 2019). This process so often focused on alginate gels loaded with cells being printed, but there is no reason why cold-set hydrogels could not be printed in this manner, with gelatin having been utilised as a support material (Jin, Compaan, Bhattacharjee, & Huang, 2016). However, this process requires the presence of the fluid gel bath, with fluid gels normally requiring equipment capable of delivering shear while controlling temperature such as a rheometer or a pin stirrer vessel (David A. Garrec & Norton, 2012). This makes it more impractical if 3D printers were to become ubiquitous within homes and healthcare settings. Furthermore having laymen handle more complicated tasks such as removing the remaining support fluid gel could also be a barrier to uptake of this method. Whereas, hot extrusion 3DP will produce finalised products that are immediately ready for use and will not require a constant supply of fluid gel.

Owing to the fact that hot extrusion hydrogel printing requires rapid thermal gelation and a high storage modulus (Diañez, et al., 2019). κC and agar are considered suitable for hot hydrogel 3DP and have been the focus of most studies in this field. κC is a sulphated polysaccharide that is extracted from red seaweed. When added to water it has the ability to form thermo-reversible gels in the presence of complementary gelling cations (Hermansson, Eriksson, & Jordansson, 1991). Its gelation is believed to occur through the ordering of randomised coils into double helices and then the aggregation of these helices into a polymeric network (Norton, Morris, & Rees, 1984). Agar is a polysaccharide that is extracted from agarophyte seaweeds. Although like κC it is as able to form thermo-reversible hydrogels, agar does not require any crosslinkers, it forms physical gels simply through hydrogen bridges; and as such it is uncharged. Agar contains two fractions, agarose and agaropectin with only agarose responsible for gelation (Armisen & Gaiatas, 2009). Both of these polysaccharides have many uses in foods as rheology modifiers and gelling agents (Saha & Bhattacharya, 2010). Vitamin B1 also known as thiamine is a water soluble essential vitamin. It is on the WHO list of essential medications and deficiencies can lead to Wernicke-Korsakoff syndrome and may arise from alcoholism or malabsorption (Kril, 1996).

While agar and κC are widespread within the food sector, they are also used as drug delivery systems as well, in part due to the biocompatibility of these hydrogels (Nayak & Gupta, 2015; Weiner, 1991). Research has gone into modified release oral dosing (Ito & Sugihara, 1996; Picker, 1999), parenteral preparations (Santoro, et al., 2011; Zhang, Tsai, Monie, Hung, & Wu, 2010) and patches applied directly to the skin (Dalafu, Chua, & Chakraborty, 2010). One of the major issues with the centralised, large scale production of medications is that doses are decided on how many people from clinical trials saw the most benefit at that dose. This can lead to people receiving too much or too little of a medicine despite being given a clinically appropriate dose (Cohen, 1999). This is why 3DP of hydrogels is considered suitable to produce customisable delivery vehicles for medicines tailored to the individual patient at the point of delivery (Fina, et al., 2018; Long, et al., 2019). However, 3DP of hydrogels is suited best for smaller batches that require high levels of customisation, whether this is for printing medicines or implant devices (Ventola, 2014). Furthermore there is still an issue with a limited range of materials currently available (Ngo, Kashani, Imbalzano, Nguyen, & Hui, 2018). While studies such as this one aim to address this issue, there is still some way to go. Finally, there will have to be widespread training in order to familiarise medical professionals at the point of production or delivery in the use of 3D printers (Choonara, du Toit, Kumar, Kondiah, & Pillay, 2016; Ventola, 2014).

This study aimed to evaluate the suitability of hydrogels for hot extrusion 3DP and compare and contrast the physical properties of printed gels to cast gels, before assessing them both as release vehicles. Because, there exists little literature on the interactions of thiamine with agar and κC, and none looking into how thiamine might affect the microstructure of the hydrogels, the first step was to characterise the thermal characteristics of the κC-thiamine and agar-thiamine hydrogels. Rheology and differential scanning calorimetry were used to determine which formulations were suitable candidates for hot extrusion 3DP. κC and agar were chosen for printing because of their desirable gelling characteristics. Thiamine was chosen as a model molecule because it has been used in release studies before (Kevadiya, et al., 2010). After suitable thiamine containing hydrogel systems were established then 3D printing under several parameters took place. The printed gels' physical properties was ascertained through texture profile analysis and light microscopy and then compared to cast gels. This highlighted the variances in the structures fabricated between the two production methods. Finally the printed and cast gels underwent release tests to assess their performances as release vehicles in water. This allowed this study to examine physical

differences between printed and cast hydrogels and show compare the performance of 3DP hydrogels to cast gels as drug delivery vehicles.

2. Materials and methods

2.1. Materials

κC, agar and sodium chloride were purchased from Sigma-Aldrich (UK). Thiamine hydrochloride 99% (hereafter referred to as thiamine) was purchased from Alfa Aesar (UK). Sodium hydroxide 1M was purchased from Honeywell and was used for pH adjustment. Milli-Q water was used (Elix® 5 distillation apparatus, Millipore®, USA) for sample preparation. All materials were used without further purifications or modifications.

2.2. Hydrogel Preparation

Samples of κC hydrogels were prepared by dispersing 3% w/v of κC into deionised water. First, a hotplate was set to 80˚C and then the water was placed on top of it in a 250mL beaker. A magnetic stirrer was used in order to facilitate dispersion and hydration of the κC into the water. After adding the κC powder into the water, it was left to stir for sixty minutes. Agar hydrogels were produced by placing 2% w/v agar into deionised water. This was then covered and placed in an 800W microwave and heated for ninety seconds until the agar melted into the water. After sixty seconds the microwave was stopped and the beaker was shaken gently. After this the solution was stored on a hotplate set to 70˚C and stirred by a magnetic stirrer.

2.3.Thiamine hydrogel preparation

For agar samples containing thiamine, the same methodology used in 2.2 was followed. However, thiamine at the required concentration (0.1%, 1%, 2% and 5% w/v) was added and then the pH was balanced back up to 5.5 using sodium hydroxide 1M and the solution was then held at 70˚C until it was ready to be used. This pH was chosen as agar did not undergo acid hydrolysis at this pH (Phillips & Williams, 2000) and the thiamine was still stable at this pH and temperature (Arnold & Dwivedi, 1971). For κC samples containing thiamine, first the thiamine was added to water and then the pH was adjusted to pH 5.5 once more to protect both the thiamine and the κC from degradation. Owing to the fact that sodium ions affect gel strength of κC hydrogels (Hermansson, et al., 1991) the exact amount of sodium hydroxide added for each concentration of thiamine was calculated from the amount of 1M sodium hydroxide added. The amount of sodium ions added to the highest concentration of thiamine was calculated to be 546 mg. Therefore, the 0%, 0.1%, 1% and 2% κC-thiamine gels had sodium chloride added to them to ensure they all contained 546 mg of sodium ions. This ensured any changes to the gel strength alone came from the thiamine and not the sodium ions.

2.4. Rheology

Rheological analysis of the samples were carried out using a modular compact rheometer 302 (Anton Paar, Austria), using parallel 50 mm sandblasted plates or 20 mm serrated plates. A working gap of 1 mm was used for all measurements. All samples were covered with silicone oil around the edges to minimise evaporation during testing. Temperature sweeps were carried out at a fixed frequency of 1 Hz within the linear viscoelastic region. The sweeps ran from 70˚C to 20˚C except for 5% w/v thiamine and κC which was carried out from 80˚C to 20˚C owing to the far higher gelling point of the system. This helped to prevent errors whereby the rheometer gave the initial storage modulus (G') as higher than the initial loss modulus (G'') despite being above the sol-gel transition temperature. Temperature sweeps were carried out at a scanning rate of 1˚C min^{-1} to be in line with previous studies (S. Liu & Li, 2016; Tomšič, Prossnigg, & Glatter, 2008). Information from the temperature

sweeps gave data on G', G'' and the phase angle (tan δ). From this information it was possible to determine the gelling (T_{gel}) and melting (T_{melt}) temperatures of the gels as the point where G' and G'' cross over (Djabourov, Leblond, & Papon, 1988).

2.5. Micro differential scanning calorimetry

Micro differential scanning calorimetry (μDSC) was carried out using a Seteram MicroDSC 3 evo (Seteram, France). This involved analysis of the thermal transitions of the tested hydrogels. 0.6-0.8 g of sample was loaded into a stainless steel cell. Then the reference cell was filled with the equivalent amount of deionised water ± 0.005 g. Samples were then subjected to the following measurement conditions used in previous studies (Brenner, Wang, Achayuthakan, Nakajima, & Nishinari, 2013; Iijima, Hatakeyama, & Hatakeyama, 2014).. First, they were cooled to 0˚C and held there for sixty minutes. Then they were heated up to 100˚C at a scanning rate of 1˚C per minute and cooled back down to 0˚C at the same rate. Then it was held for another sixty minutes and the cycle was repeated twice more. This gave three heating and cooling curves per run. Each different formulation was tested in triplicate in this manner, giving a total of nine cooling and heating curves per formulation (Brenner, et al., 2013; Iijima, et al., 2014). The temperature range of 0-100˚C was chosen because all thermal transitions in the tested systems occur within this range. Transition temperature was taken as the peak of the curve and were obtained by integrating the area below the baseline. Changes in enthalpy (ΔH) were also determined through this method (Iijima, et al., 2014).

2.6. 3D printing

The 3D printing system was created from a commercially available printrbot simple metal printer which was retrofitted to handle a liquid feed. This involved replacing the components which originally fed the plastic filament into the hot end. The new parts were computer-aided design (CAD) 3D printed parts (4. and 5. in Figure 1) which facilitated the use of a 10 mL syringe (1. In Figure 1) Due to the fact that there was no heating system, the syringe was insulated to prevent temperature loss. This was to maintain the sol state in order to allow the sol-gel transition to occur *in situ* such as with (Warner, et al., 2019). The syringe was then filled with the hot liquid sample and nozzles of several different internal diameters were tested (2. In Figure 1). Printing was carried out at ambient temperature which was set to 20˚C by the climate control. Several printing parameters were adjusted depending on the sample such as infill %, print speed, flow %, and layer height. The software used to control the printer was cura software which is freeware available online. Previous works have shown that varying these parameters can have a major impact on the outcome of print fidelity in food systems (C. Severini, et al., 2018; Fanli Yang, Zhang, Bhandari, & Liu, 2018). This proved to be true in this case with many failed prints occurring during parameter optimisation. Printability was assessed through shape fidelity (Chimene, Lennox, Kaunas, & Gaharwar, 2016) and weight uniformity (Goyanes, Buanz, Basit, & Gaisford, 2014). If the printed shapes were close to the computer generated image and were within 5% of the average weight of the printed samples they were considered to be successful. Another risk was premature gelation on the printing bed itself, which led to the nozzle dragging through gelled material owing to the pattern of printing. Conversely, if the sol-gel transition had happened too late then the hydrogel spread across the printing bed and fail to achieve layer by layer build up (Wei, et al., 2015). Layer height has been shown to affect the final print outcome in cold extrusion hydrogel 3D printing (Carla Severini, Derossi, & Azzollini, 2016). This also held true with hot extrusion printing. If the layer height was set too high the hydrogel solution came out in drops, giving broken lines and low quality prints. If it was set too low then the nozzle dragged through the gel, yielding a low quality print. If the bed (3. In Figure 1) was too cold, the first layer set too quickly and then the print might fail as the nozzle might have scraped through the set material. If the bed was too hot, the print was of

low quality as the first layer spread across the build plate due to a failure to set quickly enough. This led to subsequent layers being deposited incorrectly and the final product not properly resembling the CAD shape. Before each print the printer bed level was calibrated manually using a 100 µm gauge. A schematic of the printer is shown in Figure 1.

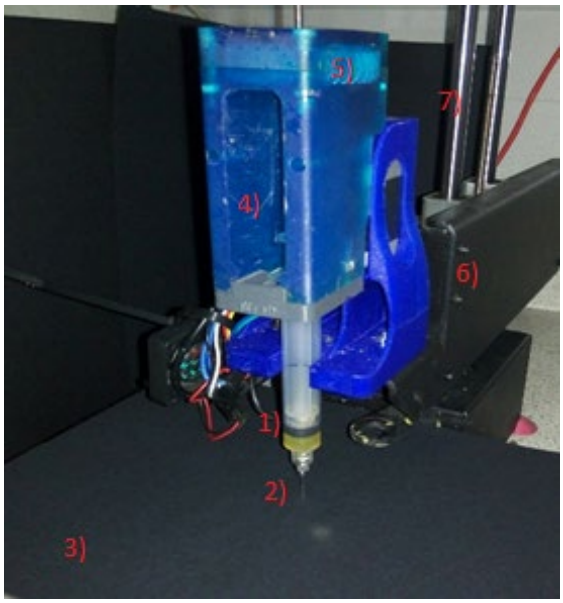

Figure 1: Schematic of the retrofitted printrbot simple metal printer including 1) Syringe to hold liquid feed, 2) Nozzle for extrusion, 3) Temperature controlled printing bed, 4) 3DP bracket to hold syringe, 5) Syringe driver for extrusion, 6) Arm to control movement in the X and Y-axes, 7) Support rods enabling movement in the Z-axis. Printer was connected to and controlled by a computer running cura freeware.

2.7. Production of moulds for casting

Moulds were produced by stereolithography 3D printing using a form 2 3D printer (Formlabs, USA). A cube and a cylinder mould were designed by CAD and uploaded to the software, this was then sliced and sent to the printer digitally to print.

2.8. Texture Profile analysis

Texture profile analysis (TPA) of the printed samples and the cast control samples was carried out using a TA XT plus Texture Analyser (Stable Micro Systems Ltd. UK) with 30 kg load cell, 3 g trigger force, P/40 (40 mm) cylindrical aluminium probe at a constant speed of 1 mm/s to match previous studies (David A Garrec & Norton, 2013). 12 mm^3 cubes and cylinders of 12 mm height and diameter were printed to be used for testing (see Figure 5.) 12mm^3 cubes and cylinders of 12 mm height and diameter were cast and used as control samples. After printing, samples were tested immediately while, for cast samples, the hydrogel solution was poured into the mould and left to gel at ambient temperature for two minutes; this was approximately equal to the printing time. Cast samples were then immediately evaluated in the texture analyser. Each test was carried out in triplicate. Through compression testing data on hardness and Young's modulus were obtained for the printed and cast samples. Hardness is defined as the peak force during the first compression cycle (Jones, Woolfson, & Brown, 1997). Young's modulus also known as elasticity, is the stiffness of the material calculated through the relationship between stress and strain of the material at low strains (Jones, et al., 1997).

2.9. Reflective light microscopy

An optical microscope (DM 2500 LED, Leica®, CH) was used to examine central cross sections of printed and cast hydrogels. The cross sections were obtained by slicing the gels thinly with a scalpel. They were then placed on a glass slide and a cover slip was placed

over the top. The microscope was set to reflective bright field settings and the software included was used to optimise the image. 4 times and 10 times magnification objectives were used. Images were captured using a charge coupled device camera (DFC450 C, Leica®, CH) attached to the microscope.

2.10 Release studies

Release studies were carried out using UV-visible spectrophotometry to assess the release of thiamine from the printed gels and compare it to that from cast gels. The gels each contained 2% w/v thiamine. Three cylinders of 12 mm height and 12 mm diameter were printed and each one was placed into a beaker containing 100mL of deionised water. Water was used as a simple, preliminary medium. In the future more complex media will be considered. Cylinders of the same height and diameter were also cast and used as control tests. Owing to thiamine's extremely high water solubility (Pharmacopoeia, 2016) this was an acceptable phase volume to obtain sink conditions (Gibaldi & Feldman, 1967). The beakers of water were put into an Incu-Shake MIDI shaker incubator (Sciquip, UK) at 100 rpm. Release tests were carried out at 20˚C in order to test out room temperature for uses other than ingestion and 37˚C for *in vivo* testing. Measurements were taken at 0, 5, 10, 15, 30, 60, 90, 120, 180, 240, 300 and 360 minutes and 24 and 48 hours. Determination of the concentration of thiamine within the dissolution medium were carried out using an Orion AquaMate 8000 UV-VIS Spectrophotometer (Thermo Fisher Scientific, UK) set to 235 nm, which was the wavelength at which the thiamine was best detected by the spectrophotometer. 20 µL of dissolution medium was taken with an eppendorf pipette and added to a 1000 µL cuvette. Then 980 µL of deionised water were added to the cuvette and the solution was homogenised in a vortex shaker for 15 seconds to be in line with previous studies (Hansen & Warwick, 1978). This was then placed into the UV-VIS spectrophotometer after it had it calibrated with a blank cuvette containing only deionised water. This gave the concentration of thiamine within the cuvette which was then adjusted to account for the total thiamine released within the dissolution medium. The release profile was calculated from a calibration curve determined by the UV-visible spectrophotometer which had an R^2 value of 0.998. The cuvette was then discarded and 20 µL of deionised water was added into each beaker. This was corrected for when calculating the thiamine concentration following the procedure of (B. Singh, Kaur, & Singh, 1997). All tests were carried out in triplicate.

2.11 Modelling of release data

Thiamine release data (up to 60%) were fitted to the model proposed by (Peppas & Sahlin, 1989):

$$\frac{M_t}{M_\infty} = k_1 t^m + k_2 t^{2m} \qquad \text{Eq [1]}$$

Where M_t/M_∞ is the fraction of active released at time t. The first term ($k_1 t^m$) relates to Fickian effects while the second term ($k_2 t^{2m}$) to relaxational contributions to the release. k_1 is the kinetic constant regarding release from the matrix by Fickian diffusion and k_2 is the kinetic constant for case-II relaxation. Lastly the coefficient m is the purely Fickian diffusion exponent which is dependent on the shape of the device (Peppas, et al., 1989); the value of the exponent concerning relaxation transport is in theory twice the Fickian exponent ($2m$). The same study further reported that the impact of each of the two mechanisms to the obtained release profile can be assessed by calculating the fractional Fickian (F) and relaxational (R) contributions from:

$$F = \frac{1}{1+\frac{k_2}{k_1}t^m} \qquad \text{Eq [2]}$$

$$R = \frac{\frac{k_2}{k_1}t^m}{1+\frac{k_2}{k_1}t^m} \quad \text{Eq [3]}$$

3. Results and discussion

3.1. Pre-printing thermal characterisation of the hydrogels

Before printing could occur it was important to establish the thermal characteristics of the gel systems. This was crucial as a strong understanding of these parameters is necessary in order to establish whether a material is printable or not. There exists virtually no literature on the effect thiamine has on the thermal characteristics of κC and agar gels. So investigations had to be carried out in order to establish if there were any changes to the gel networks following thiamine incorporation. The sol-gel transition temperature of the thiamine-biopolymer systems was determined using a rotational rheometer. This is in line with previous studies (Hermansson, et al., 1991; Watase & Arakawa, 1968) The results for average T_{gel} and T_{melt} for 3% κC and 2% agar with 0, 0.1, 1, 2 and 5% w/v thiamine are shown in Figure 2. G' and G'' for all the examined systems are presented in Figure 3.

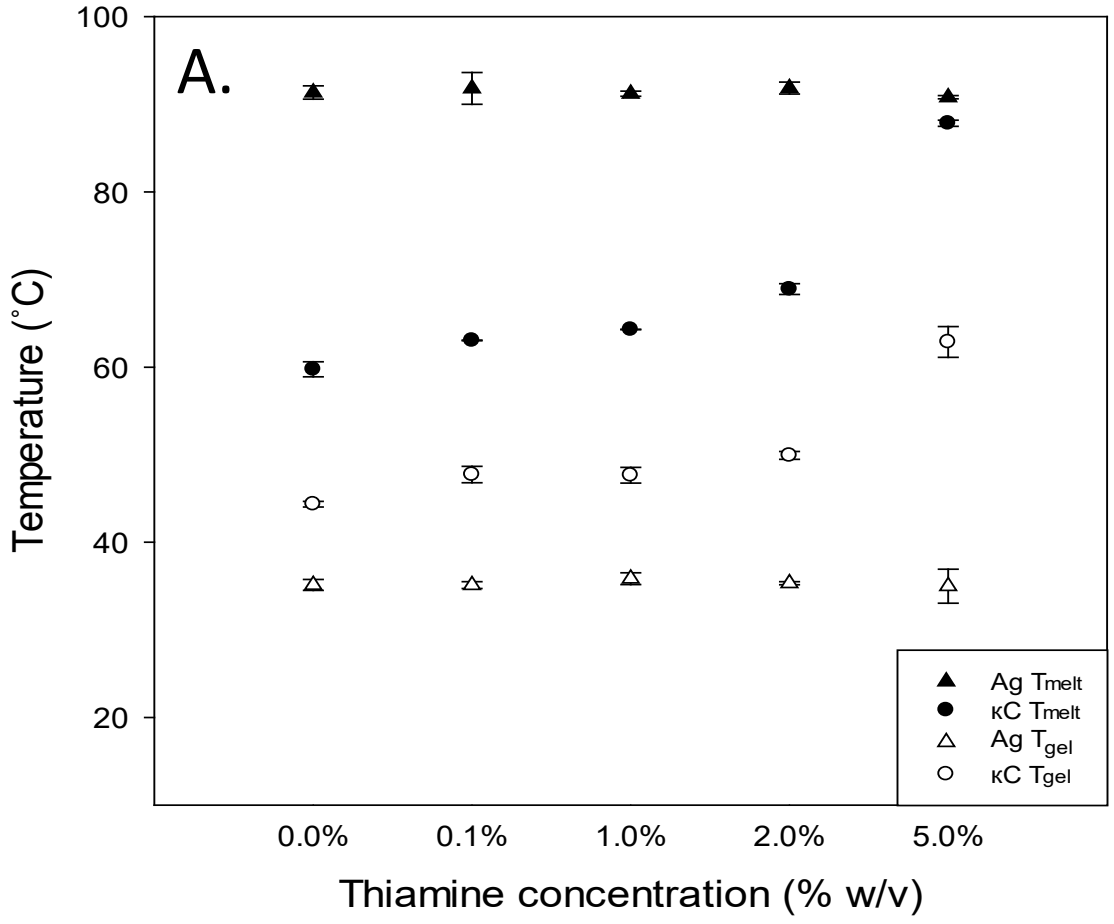

Figure 2: T_{gel} and T_{melt} of 0, 0.1, 1, 2 and 5% thiamine with 3% κC and 2% agar – Error bars are the standard deviation of the mean. n = 3

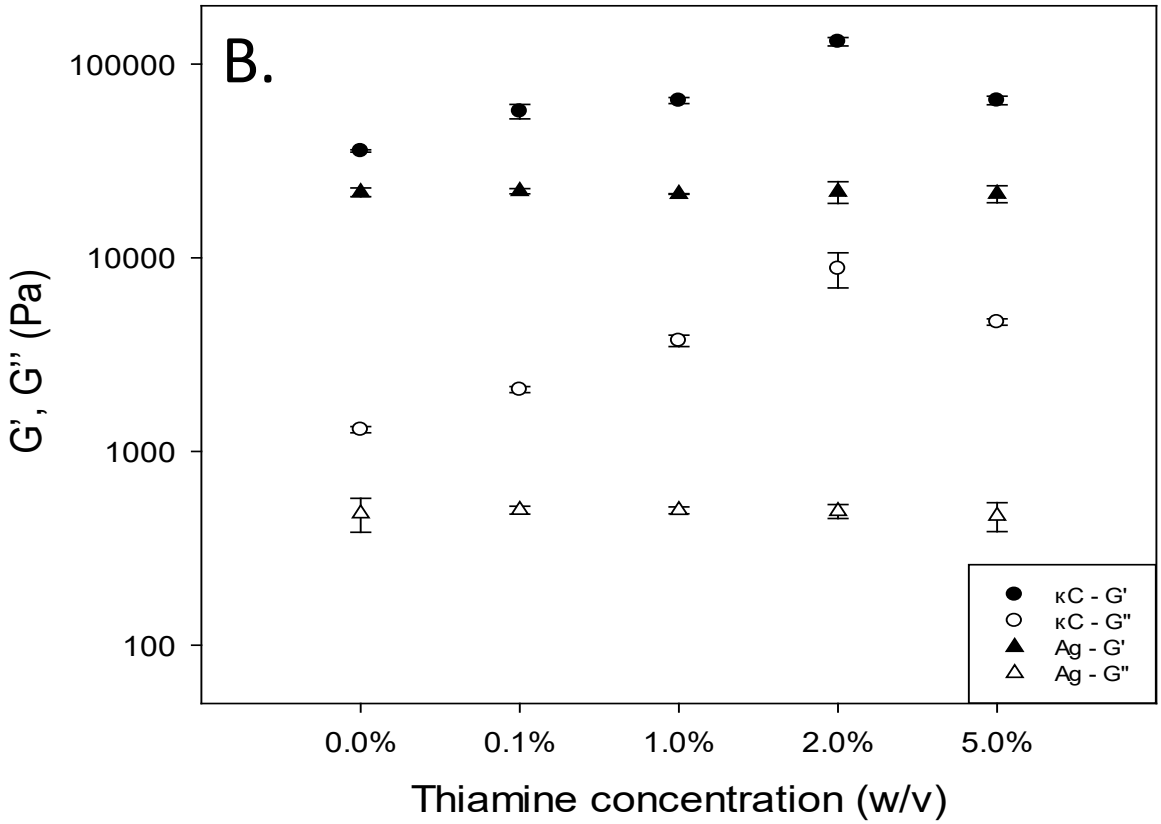

Figure 3: G' and G'' of 0, 0.1, 1, 2 and 5% thiamine with 3% κC and 2% agar

Figures 2 and 3 show that there is no interaction between the agar and the thiamine. As an uncharged molecule, agar gels through hydrogen bonding and doesn't rely on crosslinkers (Tako & Nakamura, 1988). This is reflected in Figures 2 and 3 by the transition temperatures and the moduli of agar remaining constant regardless of thiamine concentration. However, with κC and thiamine, as the concentration of thiamine increased there was a linear increase in both T_{gel} and T_{melt}. This indicates that an interaction between thiamine and κC was occurring with the transition temperatures increasing with the concentrations of the active. After dissociating from the hydrochloride salt, thiamine is a cationic molecule and κC is an anionic molecule which relies on cationic ions for gelation (Hermansson, et al., 1991). Therefore the results from the T_{gel} and T_{melt} suggest that the thiamine is complexing with the κC and reinforcing the gel network. This phenomenon has been observed with κC and other cationic molecules such as surfactants (Grządka, 2015). However, Figure 3 shows that the reinforcement of the gel network through increasing thiamine concentration, peaks at 2% w/v thiamine. At 5% thiamine a decrease in G' and G'' were observed despite increasing T_{gel} and T_{melt}. This was probably due to the κC becoming saturated with the thiamine, which is a less effective gelling agent than ions such as potassium and sodium. This led to a decrease in the aggregation of double helices which are essential to normal κC gelation. The formation of these thiamine-κC complexes caused charge cancellation and therefore hydrophobic domains which will increase the transition temperatures and inhibit gelation. This has been shown before with cationic compounds reducing gelation of κC and even preventing it when they are solely present (Norton, et al., 1984).

However, rheological results alone are not enough to conclusively show that the complexation of κC and thiamine is occurring. The same systems were tested using a DSC as well. This reaffirmed the transition temperatures and gave information on the gelling and melting enthalpies of the systems as well. Figure 4A shows the T_{gel} and T_{melt} for the thiamine-biopolymer systems. Figures 4B and C show the gelling and melting enthalpies.

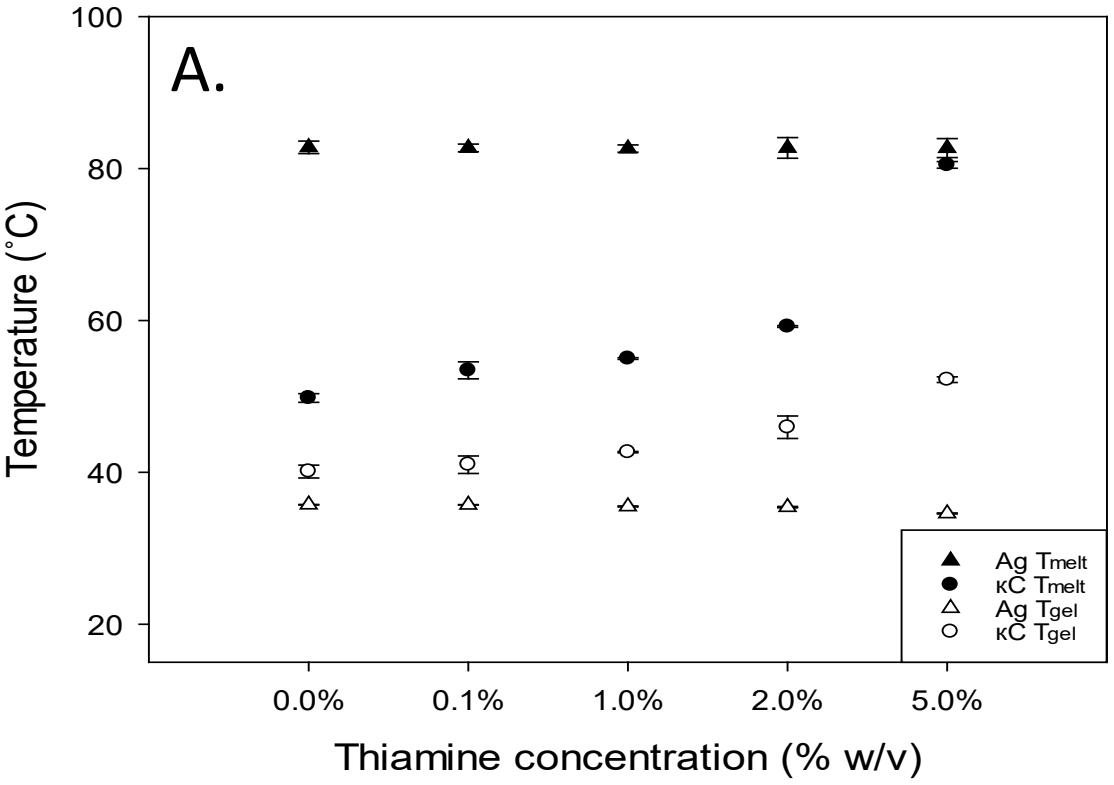

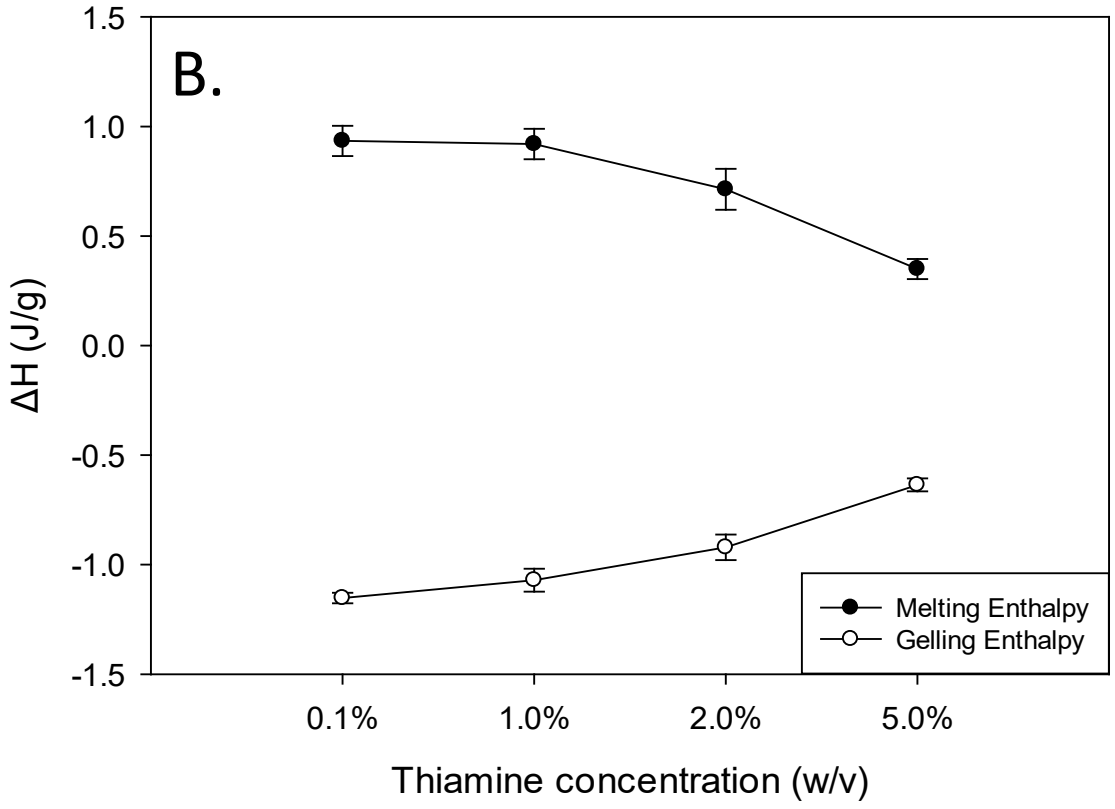

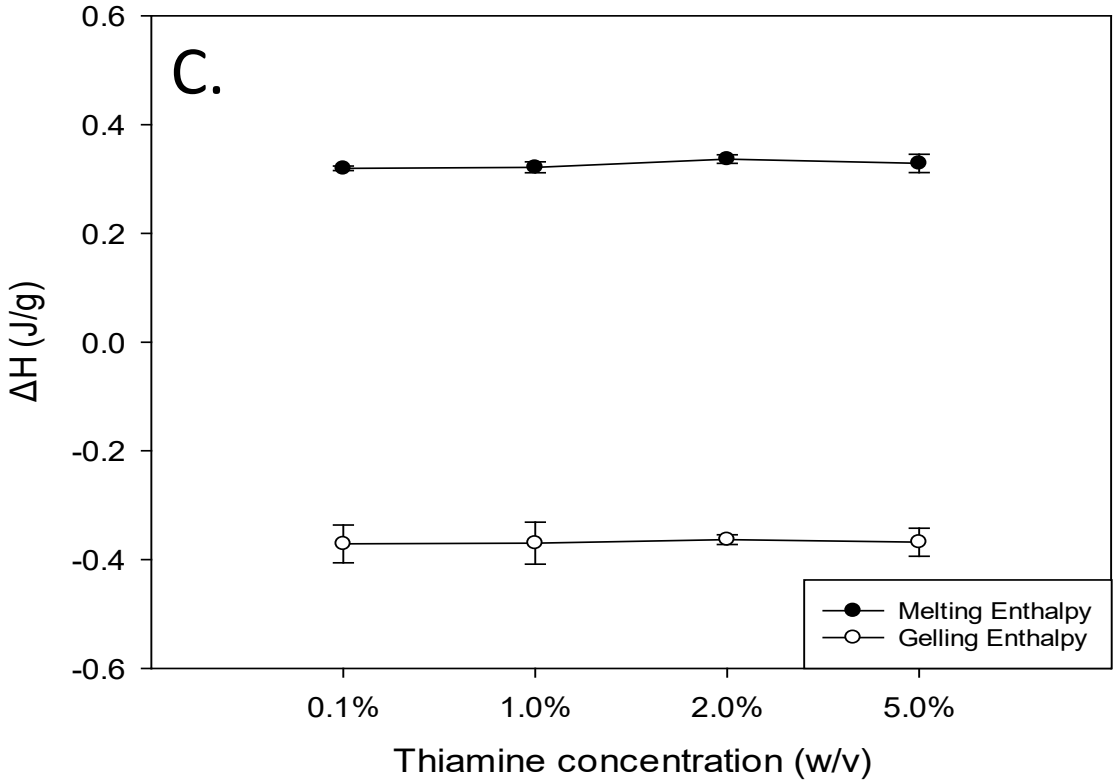

Figure 4: DSC data for the average thermal transition temperature of κC- and agar-thiamine gels (A) and the gelling and melting enthalpies of κC-thiamine (B) and agar-thiamine (C) gels.

The T_{gel} and T_{melt} for the thiamine-biopolymer systems were in agreement with the results from the rotational rheometer. While they do return somewhat different results, this is to be expected owing to the different ways in which they assess the coil to helix transition and vice versa. The rheometer and the DSC are sensitive to different parts of the gelation process of the hydrogels and the results are therefore not obtained from the same segment of the gelling mechanism (Nishinari, 1997). Again, the μDSC results for the thiamine-agar systems confirmed that no interaction is taking place between the agar and the thiamine, with constant transition temperatures and enthalpies recorded regardless of thiamine concentration. However, with the κC, the thiamine concentration had a negative correlation with the gelling and melting enthalpies. The decrease in enthalpy values indicated that there was a reduction in the amount of free sulphate groups on the backbone available for formation of electrostatic bridges with gelling cations (Rosas-Durazo, et al., 2011). Oversaturation with K^+ ions has been shown to lead to the disruption of κC cross-linking and prevention of the aggregation of double helices (Thrimawithana, Young, Dunstan, & Alany, 2010), and this phenomenon is believed to occur within these systems. The thiamine-κC hydrogels also became visually more turbid with increasing thiamine concentrations, suggesting the formation of larger complexes which were able to scatter light.

3.2. Hydrogel printing

The samples chosen for printing were those that had a higher storage modulus and exhibited rapid solidification (Li, Li, Qi, Jun, & Zuo, 2014). A higher storage modulus has been shown to produce printed products with better shape retention (Costakis, Rueschhoff, Diaz-Cano, Youngblood, & Trice, 2016). The thermal characterisation identified that hydrogels with a 2% thiamine concentration were best suited for 3DP, as it gave the highest storage modulus and gelled rapidly for the κC. The agar was the same regardless of the

thiamine concentration so 2% was also used. The parameters tested for the 3D printing of κC-thiamine hydrogels are shown in table 1 below.

Table 1: A table showing the different parameters tested in the hydrogel 3D printing process

NS	H_L (mm)	Flow (%)	T_{PB} (°C)	v_p (mm/s)	T_H (°C)	3D Outcome and Comments
18G	1.4	50	40	30	80	Under extrusion – Set too slowly
18G	1.4	60	45	30	75	Under extrusion – Set too quickly
18G	1.4	70	45	20	75	Over extrusion – Set too slowly
20G	1	35	40	20	75	Slight under extrusion – Set properly – nozzle dragged through shape
20G	1	40	40	20	75	Sufficient extrusion – Set properly – nozzle dragged through shape
20G	1.2	35	40	20	75	Slight under extrusion – Set properly
20G	1.2	35	40	20	80	Slight over extrusion – Set properly
20G	1.2	40	40	20	70	Slight under extrusion – Set properly
20G	1.2	40	40	20	75	Sufficient extrusion – Set properly
20G	1.2	40	40	20	80	Over extrusion – Set properly
20G	1.2	45	40	20	75	Slight over extrusion – Set properly
20G	1.2	50	40	20	75	Over extrusion – Set too slowly
20G	1.4	35	40	20	75	Under extrusion – Set properly
20G	1.4	40	40	20	75	Under extrusion – Set properly
20G	1.4	45	40	30	75	Over extrusion – Set properly – nozzle dragged through shape
20G	1.4	50	45	20	80	Over extrusion – Set too slowly
22G	1.4	30	40	20	60	Under extrusion – Set too quickly
22G	1.4	40	45	30	75	Under extrusion – Set too slowly
22G	1.4	50	50	40	80	Over extrusion – Set too slowly

NS: Nozzle size

H_L: Layer height (mm)

Flow: Flow percentage (%)

T_{PB}: Printer bed temperature (°C)

v_p: Print speed (mm/s)

T_H: Hold temperature (°C)

The printing parameters from table 1 that yielded the highest quality and most repeatable prints for thiamine-κC hydrogels were a 20 gauge nozzle, layer height 1.2 mm, flow percentage of 40%, printer bed temperature 40˚C, print speed of 20 mm/s and a hold temperature of 75˚C.

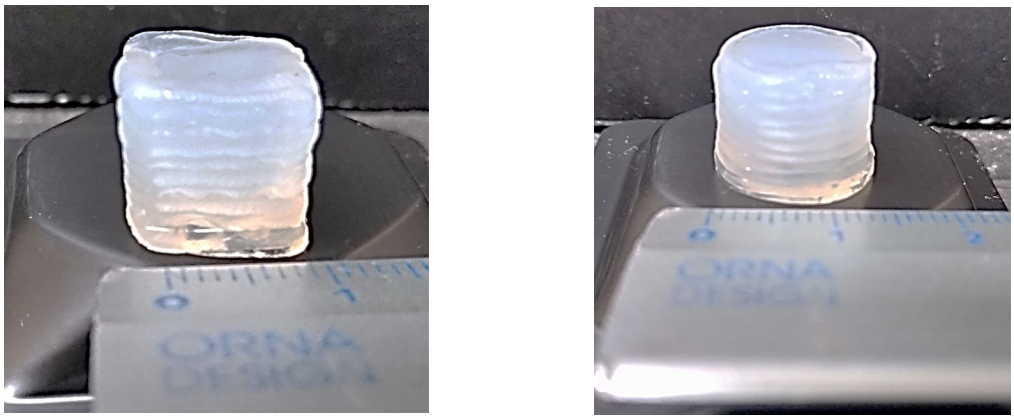

Figure 5: 3D printed 12 mm cube (A) and 12 mm height and diameter cylinder (B) printed using 3% κC and 2% thiamine hydrogel

The agar was unable to successfully print under all tested conditions. This was believed to be because the agar-thiamine hydrogels with their far lower G' of 20,000 pascals had poorer shape retention compared to the κC-thiamine hydrogels which had a G' of around 120,000 pascals. Agar's lower T_{gel} of around 37˚C might also have been a contributing factor as well. This meant that there was less of a temperature differential between the T_{gel} and printing temperature. This led to a slower gelation time and poorer shape fidelity, with the shape unable to hold the weight of subsequent layers. Too much spreading also meant that the nozzle dragged through the hydrogel solution, distorting the shape. The reasons for failure might also have been due to limitations with the printer hardware, as a lack of temperature control on the syringe meant that the hydrogel solution could not be held just above its T_{gel}. Other modifications such as a cooling fan might also have yielded improved results. Finally changes to the formulation such as increasing the concentration of the agar or addition of an adjunct such as sucrose to increase gel strength and temperature could be successful in future (Normand, 2003). Therefore going forward only thiamine-κC gels were used.

3.3. Post-printing texture profile analysis of the hydrogels

TPA of gels is often used to assess their microstructure performance and how this affects specific functionality, including their ability to deliver therapeutic molecules (Özcan, et al., 2009). With the layer by layer nature of 3D printing, the 3D printed structures have a different internal structure compared to a cast/moulded structures (Padzi, Bazin, & Muhamad, 2017). However, there is not much literature that compares 3DP hydrogels to their cast equivalent, and thus TPA was used to begin understanding and characterising some of the internal differences. Figure 4 shows the data obtained for the hardness and Young's modulus of printed and cast cubes and cylinders.

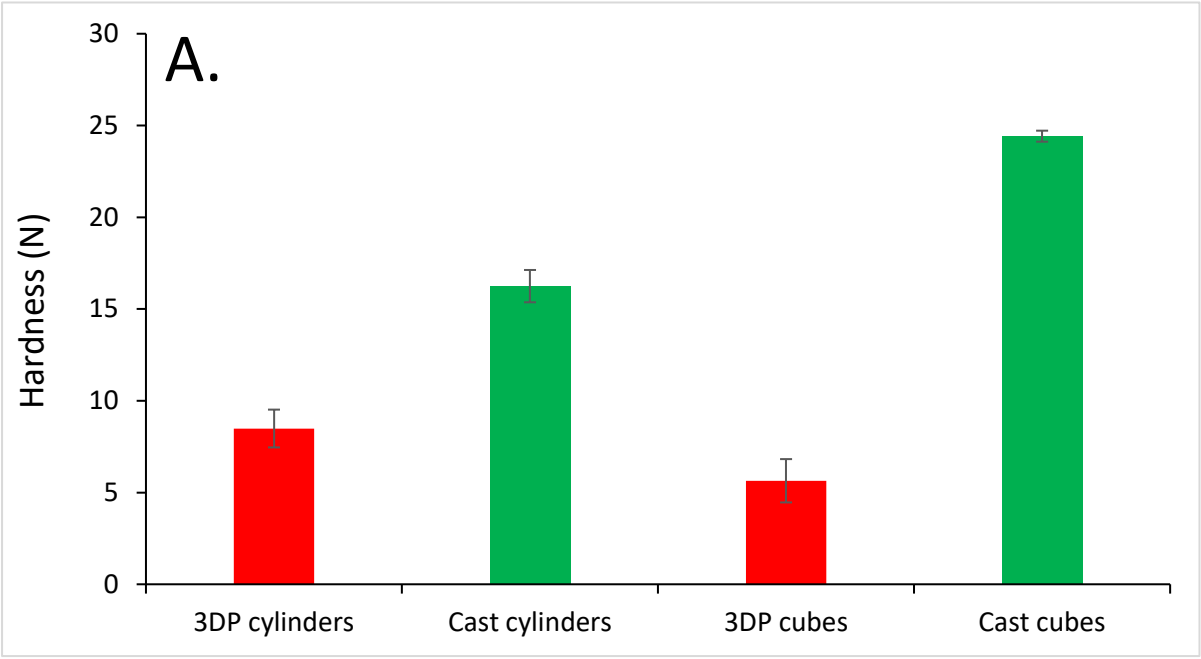

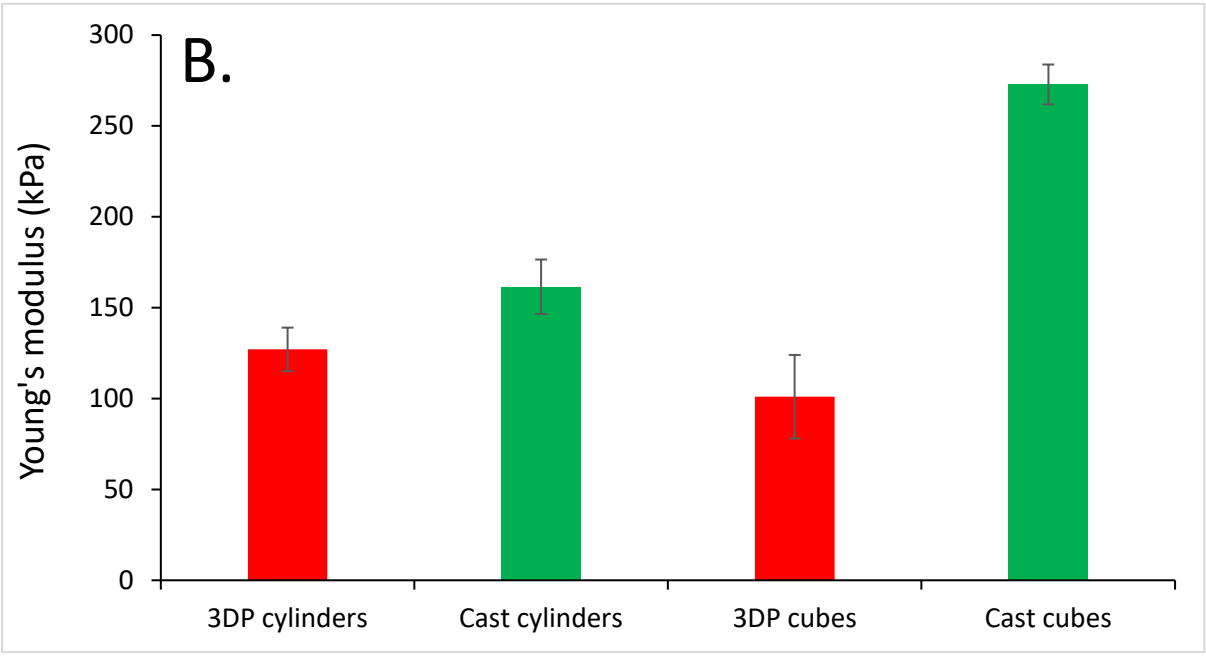

Figure 6: Hardness (A) and Young's modulus (B) of the printed and cast cubes and cylinders

The results obtained from the TPA are much higher than those observed in literature (Artignan, Corrieu, & Lacroix, 1997; David A Garrec, et al., 2013) which is due to both the higher concentration of κC used and the addition of the Na+ ions and the thiamine reinforcing the gel network as discussed. The TPA data highlights the differences in the bulk structure of a printed gel compared to a cast gel. The higher hardness value shows that the continuous cast gel network is much more robust. The TPA showed that the cast samples were stiffer than the printed samples when undergoing compression. It was also noted that cubes were harder and less elastic than the cylinders for the cast samples. The cubes had a cross-sectional surface area of 144 mm^2 and a volume of 1728 mm^3. The cylinders had a cross-sectional surface area of approximately 113 mm^2 and a volume of 1357 mm^3. There exists almost no literature comparing cubes to cylinders of the same material subjected to

compression tests, within the range of materials studied, however it has been shown that variations in surface area can affect results obtained from TPA (Rosenthal, 2010). Since gels printed in this manner are in effect a discontinuous network, with several small networks only semi fused, the TPA showed they are less resistant to the external damage owing to the differences in the structure. Figure 7 shows a cube that has undergone compression testing. The printed shapes delaminated rather than fracturing like a cast gel. Since this was occurring rather than a fracture, the bonds holding the layers together must have been weaker than the gel network itself. Since the cast gels were one continuous network, they therefore could resist greater amounts of force as shown by the TPA results.

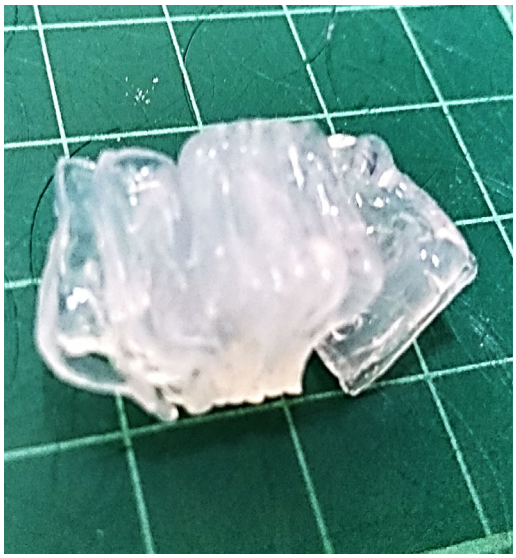

Figure 7: A printed 12 mm κC-thiamine hydrogel cube that has delaminated after undergoing compression testing

3.4. Post-printing light microscopy of the hydrogels

While the separate printed layers could clearly be seen when observing the printed shapes with the naked eye, when cutting a central cross-section they were no longer discernible. It was important to establish whether the shapes had had some of the layers fuse together or whether the printed shapes were a series of individual gel networks held together by physical bonds. FDM printed plastics have been shown to have gaps running through the structure as a consequence of the manufacturing technique (Sood, Ohdar, & Mahapatra, 2010). The presence of these gaps running through the printed shapes could affect the final release profile of the thiamine by creating a shorter diffusion path. It also helped to confirm the findings from the TPA as the internal structure differed from that of a cast gel network. The differences in internal structure were responsible for overall different bulk structure. Figure 8A and B show the outside of a cast cube and a printed cube respectively. The ridges observed in 8B are due to the printing process and show a clearly different external structure to the cast cube. Figure 8C and D show a central cross-section from a cast cube and a printed cube. This highlights the stark differences in the structures created by 3DP and casting when it comes to hydrogel production. Figure 8D presented that 3DP produced hydrogels have visible layering running through them as indicated by the lines visible in the image. Figure 8C showed cast gels with a homogenous, continuous structure as was expected. This layering is believed to affect the physical characteristics of the gel as determined in the TPA.

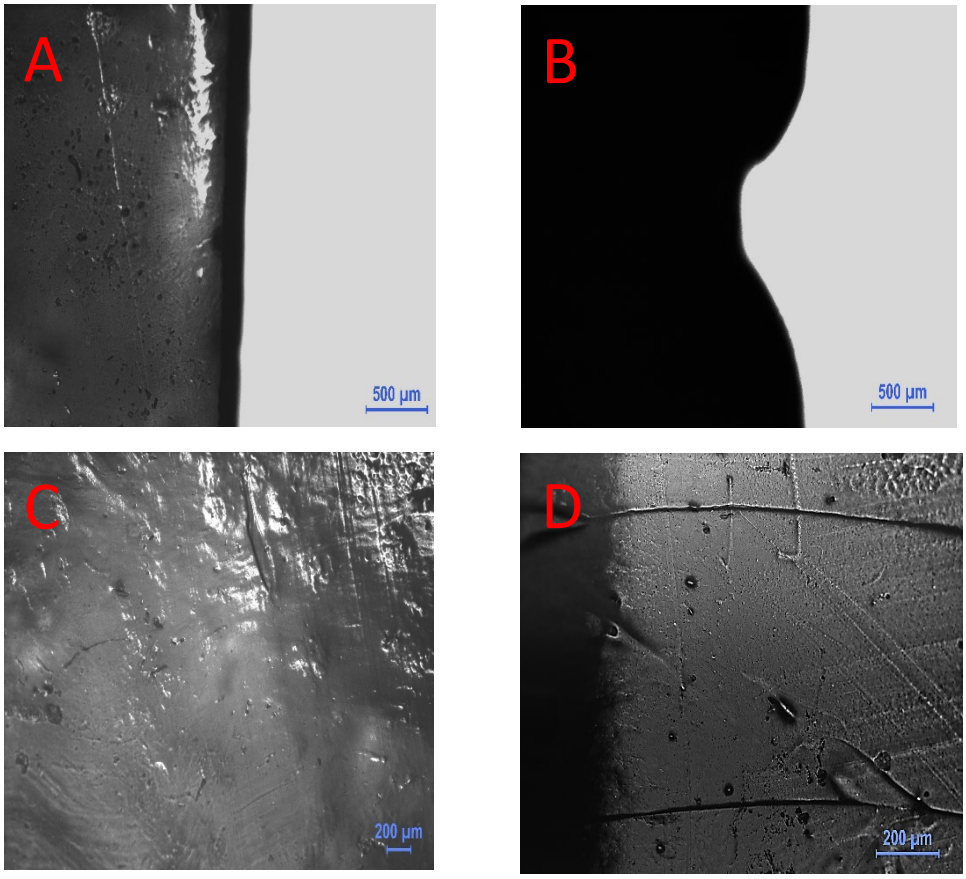

Figure 8: Microscope images of cast (A) and printed (B) κC-thiamine hydrogels from the outside layer, and cross-sections of cast (C) and printed (D) κC-thiamine hydrogels

3.5. Hydrogel release studies

There exists very little literature comparing the release rate from 3DP and traditionally manufactured structures. 3DP capsules have been shown to released dye at the same rate as injection moulded capsules (Melocchi, et al., 2015). However, these were only 0.3 mm in width and hollow, so this might not be applicable to the shapes studied which were far thicker and solid throughout. The amount of thiamine released from the printed and cast cylinders was assessed at 20˚C and 37˚C and the obtained release profiles are shown in Figures 9A and 9B respectively. Cubes were not selected for release testing as the chosen model for analysis does not account for this shape (Peppas, et al., 1989). All of the cylinders both printed and cast weighed 1.45 g ± 5%. Release of the active increased from 20˚C to 37˚C due to increased energy in the system facilitating a greater rate of release by diffusion (Vrentas & Vrentas, 1992). However, diffusion might not be the only factor in effect. Release of an active from a polymer matrix can also be dependent on relaxation of the polymer matrix as well as Fickian diffusion (Peppas, et al., 1989). The release data also showed a difference in the release rates between the printed and the cast gels. At both temperatures the printed gels showed an increase in initial release rate over the first fifteen minutes as shown by Figure 9C when compared to the cast gels. Moreover, the release data showed that there was a greater amount of thiamine released from the printed cylinders after 360 minutes compared to the cast ones.

Figures 9A and 9B showed that the cast cylinders released less thiamine over six hours at both of the tested temperatures compared to the 3D printed cylinders. Therefore, structural and mechanical differences between the two types of gel system must also contribute to the different release rates. In hydrogels, the physical characteristics determined from TPA such

as hardness have been shown to affect molecular release (Jones, Woolfson, Djokic, & Coulter, 1996). This was observed to occur in this study as well with the printed samples having lower values for hardness compared to the cast samples. Also, the elasticity seemed to have no effect on the release in their study with the elasticity values for the highest and lowest releasing systems being within 0.04 of each other on average. This indicates that while the TPA data might go some way in explaining the differences in release rate, it is not absolute. The layers running throughout the printed shapes lead to a decrease in the diffusion path as water is able to pass into the printed cylinders at a quicker rate than the cast cylinders owing to the differences in the bulk structure. This led to an increase in the release rate as shown by (Liang, et al., 2006). Furthermore, after the release tests the cast and printed cylinders had the surface water removed by drying and were weighed out, with the printed cylinders having increased on average more in weight than the cast cylinders. This further supports the notion that water was able to pass into the 3DP cylinders at a faster rate.

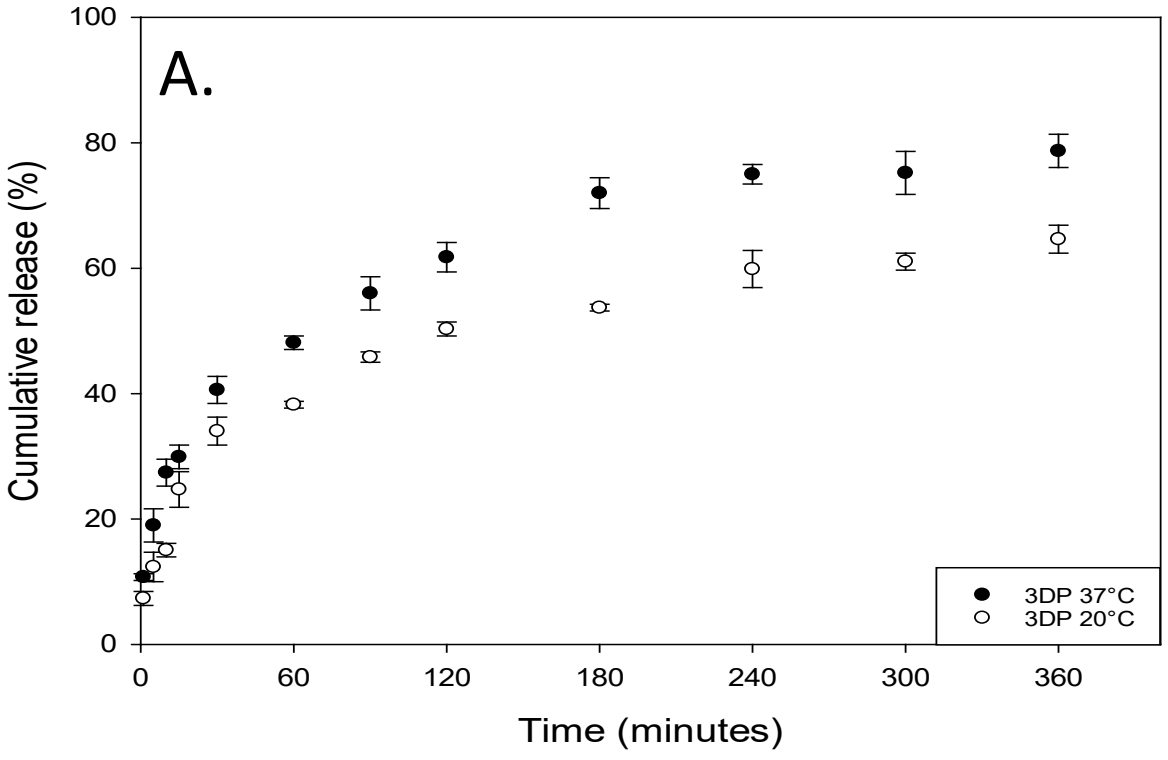

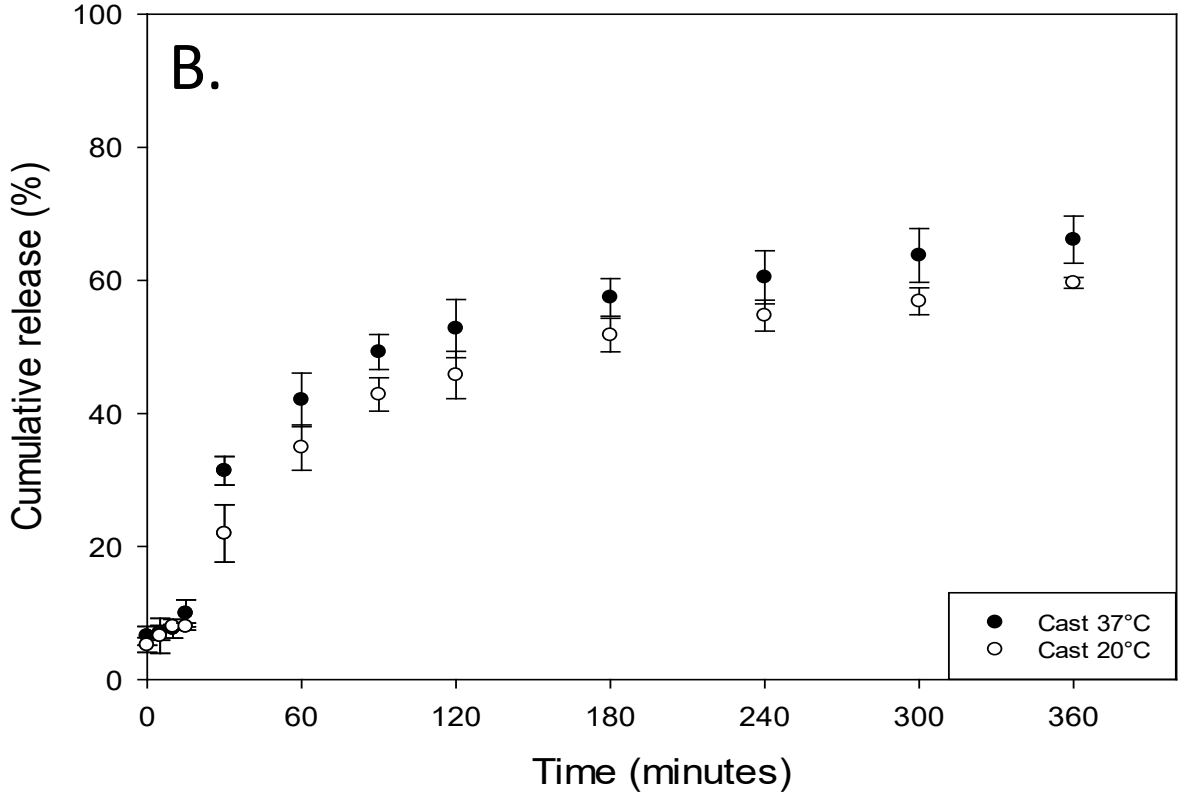

518

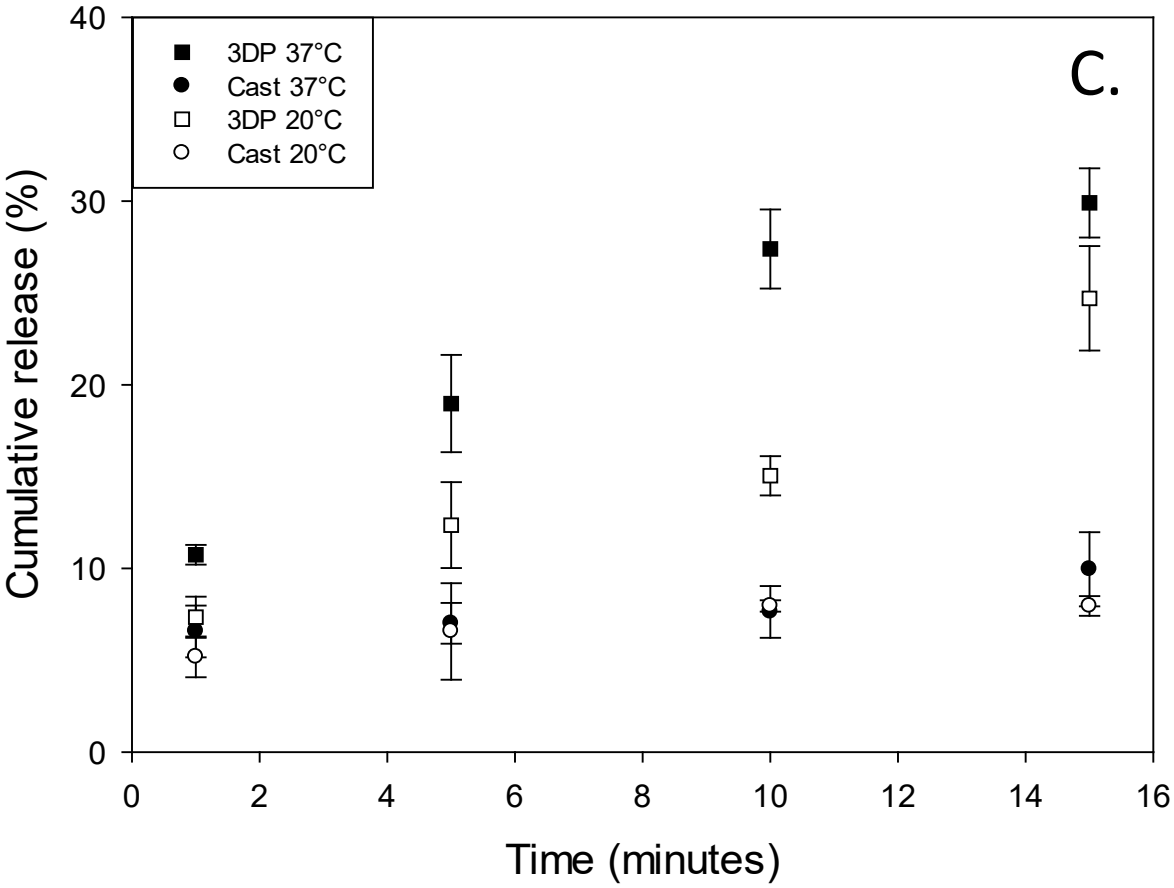

519

520 *Figure 9: A comparison of cumulative release rates of thiamine from printed (A) and cast (B) and both for the first*
521 *15 minutes (C) κC 3% and thiamine 2% hydrogels.*

The drug release profiles for the printed and cast gels at both temperatures were fitted to the Peppas-Sahlin equation. The kinetic constants for Fickian diffusion and case-II relaxational contribution were calculated through plotting the first 60% of the release data to equation 1. This made it possible to calculate F and R to the release of thiamine from the printed and cast hydrogels. The data is shown in Figure 10, with the information on k_1, k_2 *and* m available in table 2.

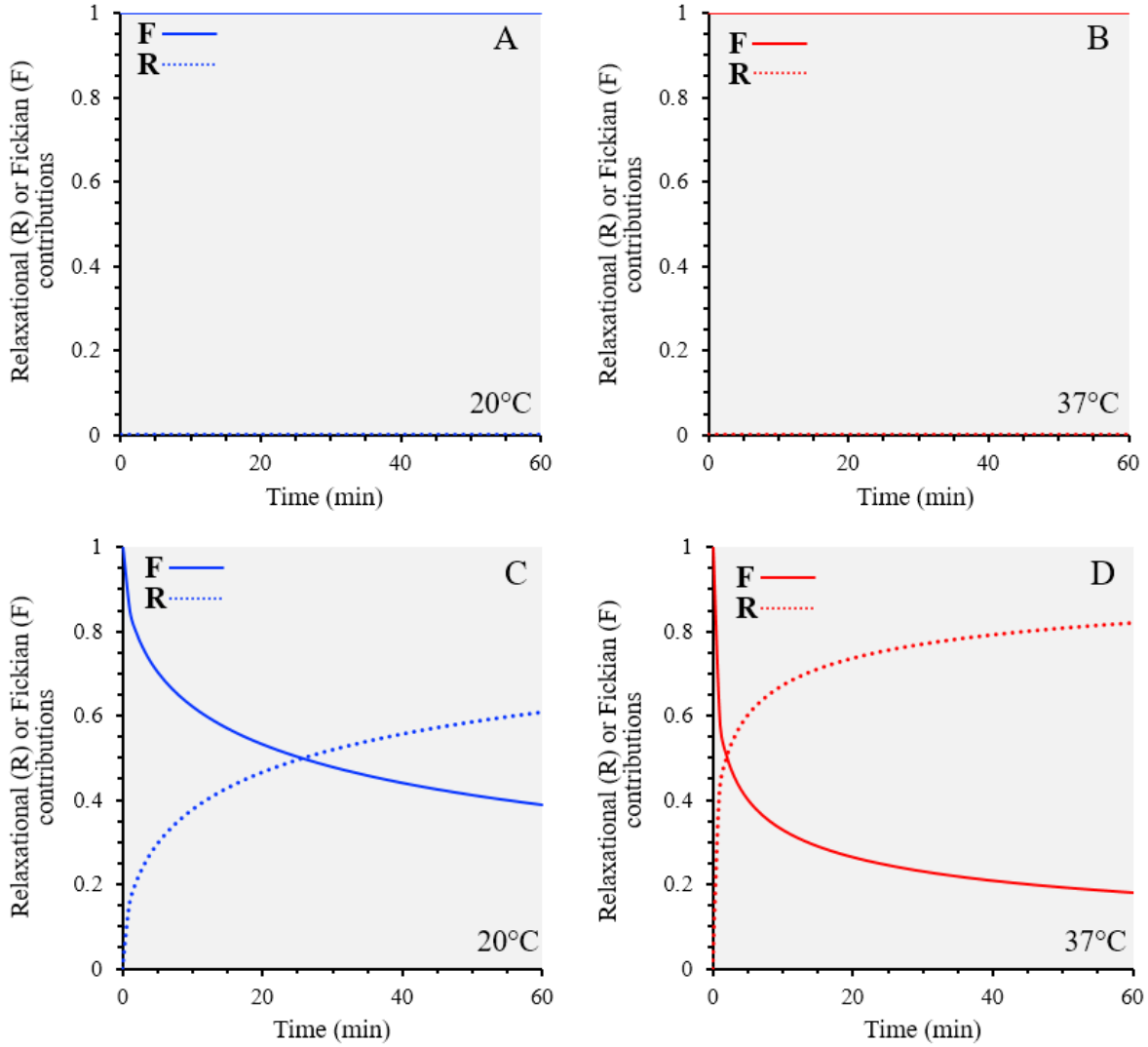

Figure 10: Data showing the percentage thiamine release due to Fickian diffusion and relaxation for printed cylinders at 37˚C (A) and 20˚C (B) and cast cylinders at 37˚C (C) and 20˚C (D)

	37˚C printed	37˚C cast	20˚C printed	20˚C cast
k_1	11.46	1.266	6.902	1.586
k_2	$8.37E^{-14}$	0.9282	$2.91E^{-9}$	0.2867
m	0.3572	0.4459	0.4321	0.5267

Table 2: The constant values used in the calculation for F and R for the release tests of the cast and printed cylinders at both temperatures

Figures 10A and 10B showed that with the 3DP shapes the diffusion contribution was essentially 100% for the printed shapes at both temperatures, with F being practically equal to 1 throughout the test. Whereas Figures 10C and 10D show that there is a relaxation contribution to the thiamine release from the cast cylinders. Both of the cast temperatures started out with diffusion being the dominant contribution. However, as the tests progressed the relaxation contribution started to exert more influence eventually becoming the dominant mechanism of release. This can be observed where the dotted line crosses the solid line. This happened more quickly at 37˚C compared to 20˚C due to there being more energy in the system. This led to a faster relaxation of the polymer chains (Watase, et al., 1968). This showed that the cast systems behaved in a manner seen in previous reports (Baggi & Kilaru, 2016) and (Lupo, Maestro, Gutiérrez, & González, 2015). However, for the 3DP cylinders it is believed that the different internal structure allowed water to penetrate faster into the shapes and so diffusion had been encouraged to such an extent as to make the relaxation contribution negligible (Falk, Garramone, & Shivkumar, 2004).

Figure 11A and B show the TPA data for the printed cylinders had a greater decrease in hardness and elasticity compared to the cast cylinders. By absorbing more water, essentially the concentration of the κC and the thiamine within the gel decreased more compared to the cast gels. This caused there to be a less dense polymer network and could have contributed to an increase in release rate (Wu, Joseph, & Aluru, 2009). Also swelling would have increased the pore size of the hydrogel (Ganji, Vasheghani, & Vasheghani, 2010), which could also have increased the release rate in this case if the pore size was a rate limiting factor (Meena, Prasad, & Siddhanta, 2007). If it was not then the swelling would not have affected the release rate (Varghese, Chellappa, & Fathima, 2014). However, even after 48 hours, neither formulation had released 100% of the thiamine into the dissolution medium. This might be because with such a high G' value, the gel network was simply so dense that not all of the thiamine was able to diffuse out despite the swelling that occurred (Patil, Dordick, & Rethwisch, 1996). However, it could also be due to the use of an incubator shaker rather than the use of a USP paddle apparatus as is usually used in release studies. Finally, the electrostatic complexation of the κC and the thiamine might also have been responsible for the failure to reach 100% release (Daniel-da-Silva, Ferreira, Gil, & Trindade, 2011). Future study needs to go into this area as well as studying different pH levels in the release media.

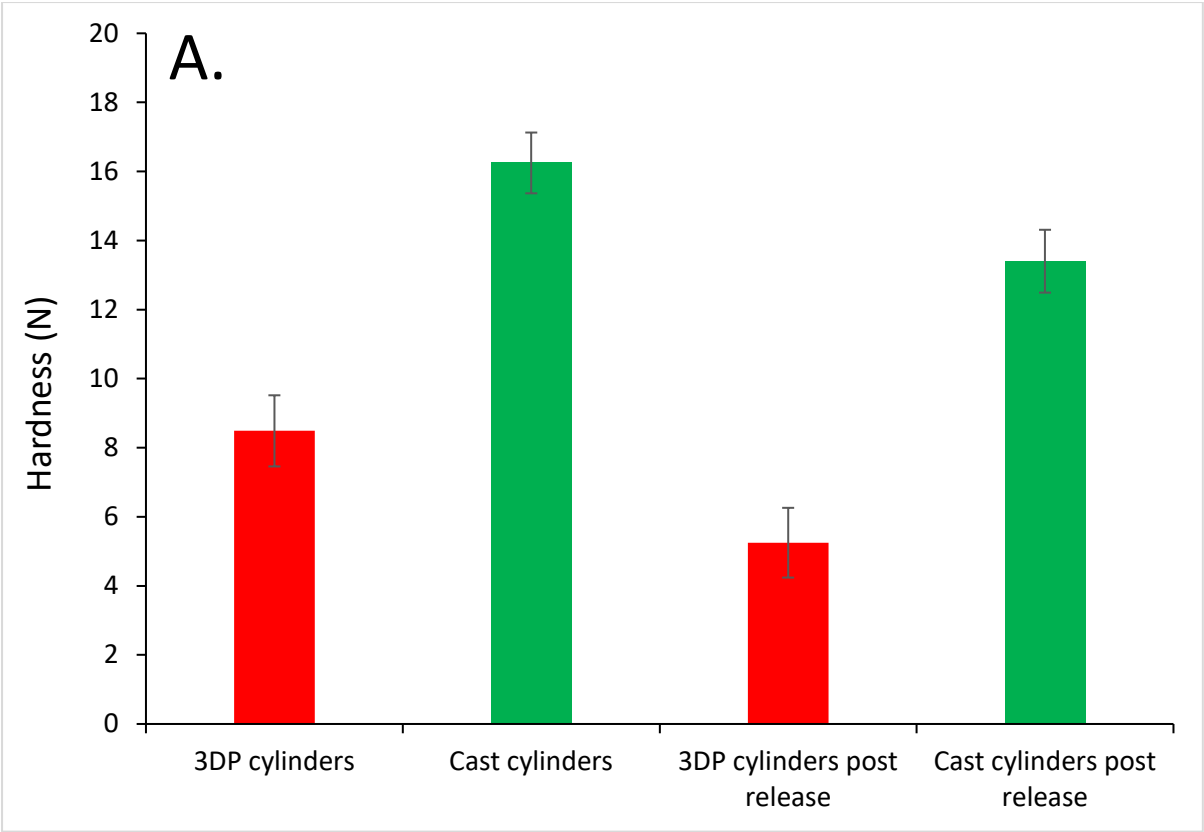

568

569

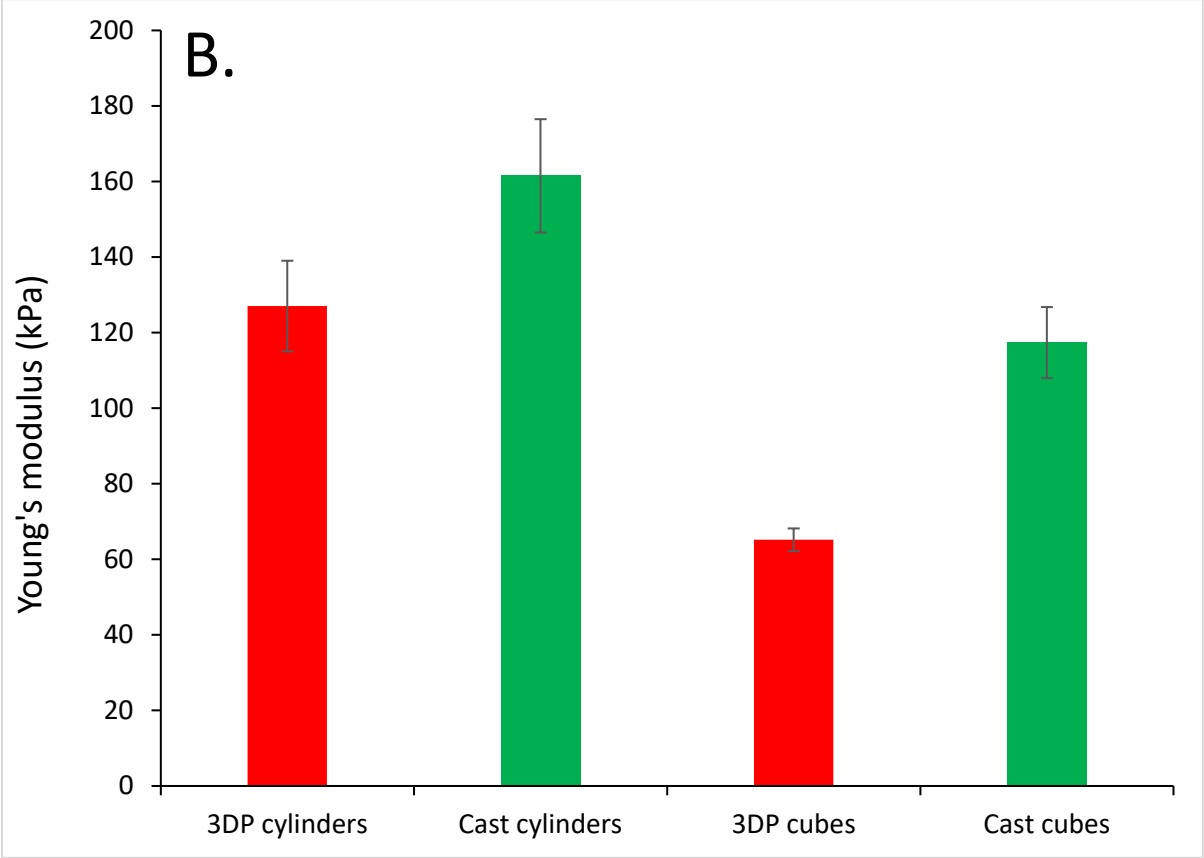

570

571 *Figure 11: Post-release study texture analysis of printed and cast gels assessing hardness (A) and young's*
572 *modulus (B)*

4. Conclusions

In this study, κC and agar thiamine-loaded hydrogels were assessed for their suitability for 3D printing. Rheological analysis showed that while thiamine does not interact with agar, it can form electrostatic complexes with κC that lead to gel structure reinforcement (up to a point). Beyond this, thiamine addition caused a marked decrease in G' while both T_{gel} and T_{melt} continued to increase. μDSC confirmed the same trends and further revealed that the gelling and melting enthalpies for κC-thiamine systems were shown to decline with increasing thiamine concentration.

2% agar was unable to print due to a lower G' and T_{gel}, but 3% κC-2% thiamine hydrogels were printable, and cubes and cylinders could be formed with reproducible weights and dimensions. The printed gels' physical properties were then compared to traditionally produced cast gels of the same dimensions and weight within a margin of ± 5%. TPA, microscopy and release studies were used to show that 3D printing facilitated the creation of gels with different physical properties without having to chemically modify the gel ingredients.

In terms of release, printed cylinders released a higher fraction of enclosed active than the cast cylinders. They also exhibited a faster rate of release over the first 15 minutes of testing. This was due to differences in the physical structure of the printed cylinders compared to the cast cylinders, which meant that printed cylinders were more prone to swelling. Modelling showed that while thiamine release from the cast cylinders was driven by both Fickian and relaxation phenomena, printed cylinders allowed the delivery of the active solely via diffusion.

Although agar was not shown to be suitable for printing under the current formulation/processing conditions, printability might still be realised at higher hydrocolloid concentrations or through the use of adjunctive materials to increase its gelation rate and G' value. Similarly, although κC hydrogels could be successfully printed, they were unable to release the entirety of enclosed thiamine, thus further flexibility in terms of active delivery could be achieved for non-interacting addenda. Nonetheless, the current study does clearly highlight the promise of hydrogel utility for formation of food-related structures via 3D-printing, capable of performing differently to cast gels of the same material.

Acknowledgements

This work was supported by the Engineering and Physical Sciences Research Council [grant number EP/N024818/1].

5. References

Armisen, R., & Gaiatas, F. (2009). Agar. In *Handbook of hydrocolloids* (pp. 82-107): Elsevier.

Arnold, R. G., & Dwivedi, B. K. (1971). Hydrogen sulfide from heat degradation of thiamine. *Journal of Agricultural and Food Chemistry, 19*(5), 923-926.

Artignan, J.-M., Corrieu, G., & Lacroix, C. (1997). Rheology of pure and mixed kappa-carrageenan gels in lactic acid fermentation conditions. *Journal of Texture Studies, 28*(1), 47-70.

Azam, R. S. M., Zhang, M., Bhandari, B., & Yang, C. (2018). Effect of Different Gums on Features of 3D Printed Object Based on Vitamin-D Enriched Orange Concentrate. *Food Biophysics, 13*(3), 250-262.

Baggi, R. B., & Kilaru, N. B. (2016). Calculation of predominant drug release mechanism using Peppas-Sahlin model, Part-I (substitution method): A linear regression approach. *Asian Journal of Pharmacy and Technology, 6*(4), 223-230.

Brenner, T., Wang, Z., Achayuthakan, P., Nakajima, T., & Nishinari, K. (2013). Rheology and synergy of κ-carrageenan/locust bean gum/konjac glucomannan gels. *Carbohydrate Polymers, 98*(1), 754-760.

Buchanan, C., & Gardner, L. (2019). Metal 3D printing in construction: A review of methods, research, applications, opportunities and challenges. *Engineering Structures, 180*, 332-348.

Chen, Z., Li, Z., Li, J., Liu, C., Lao, C., Fu, Y., Liu, C., Li, Y., Wang, P., & He, Y. (2019). 3D printing of ceramics: A review. *Journal of the European Ceramic Society, 39*(4), 661-687.

Chimene, D., Lennox, K. K., Kaunas, R. R., & Gaharwar, A. K. (2016). Advanced Bioinks for 3D Printing: A Materials Science Perspective. *Ann Biomed Eng, 44*(6), 2090-2102.

Choonara, Y. E., du Toit, L. C., Kumar, P., Kondiah, P. P. D., & Pillay, V. (2016). 3D-printing and the effect on medical costs: a new era? *Expert Review of Pharmacoeconomics & Outcomes Research, 16*(1), 23-32.

Cohen, J. S. (1999). Ways to minimize adverse drug reactions: individualized doses and common sense are key. *Postgraduate medicine, 106*(3), 163-172.

Compaan, A. M., Song, K., & Huang, Y. (2019). Gellan Fluid Gel as a Versatile Support Bath Material for Fluid Extrusion Bioprinting. *ACS applied materials & interfaces, 11*(6), 5714-5726.

650 Costakis, W. J., Rueschhoff, L. M., Diaz-Cano, A. I., Youngblood, J. P., &
651 Trice, R. W. (2016). Additive manufacturing of boron carbide via
652 continuous filament direct ink writing of aqueous ceramic
653 suspensions. *Journal of the European Ceramic Society, 36*(14),
654 3249-3256.
655 Dalafu, H., Chua, M. T., & Chakraborty, S. (2010). Development of κ-
656 Carrageenan Poly (acrylic acid) Interpenetrating Network
657 Hydrogel as Wound Dressing Patch. In *Biomaterials* (pp. 125-
658 135): ACS Publications.
659 Daniel-da-Silva, A. L., Ferreira, L., Gil, A. M., & Trindade, T. (2011).
660 Synthesis and swelling behavior of temperature responsive
661 kappa-carrageenan nanogels. *J Colloid Interface Sci, 355*(2), 512-
662 517.
663 Diañez, I., Gallegos, C., Brito-de la Fuente, E., Martínez, I., Valencia, C.,
664 Sánchez, M. C., Diaz, M. J., & Franco, J. M. (2019). 3D printing in
665 situ gelification of κ-carrageenan solutions: Effect of printing
666 variables on the rheological response. *Food Hydrocolloids, 87*,
667 321-330.
668 Diaz, J. V., Van Bommel, K. J. C., Noort, M. W.-J., Henket, J., & Briër, P.
669 (2018). Method for the production of edible objects using sls
670 and food products. In: Google Patents.
671 Djabourov, M., Leblond, J., & Papon, P. (1988). Gelation of aqueous
672 gelatin solutions. II. Rheology of the sol-gel transition. *Journal de*
673 *Physique, 49*(2), 333-343.
674 Falk, B., Garramone, S., & Shivkumar, S. (2004). Diffusion coefficient
675 of paracetamol in a chitosan hydrogel. *Materials Letters, 58*(26),
676 3261-3265.
677 Fina, F., Goyanes, A., Madla, C. M., Awad, A., Trenfield, S. J., Kuek, J.
678 M., Patel, P., Gaisford, S., & Basit, A. W. (2018). 3D printing of
679 drug-loaded gyroid lattices using selective laser sintering.
680 *International journal of pharmaceutics, 547*(1-2), 44-52.
681 Ganji, F., Vasheghani, S., & Vasheghani, E. (2010). THEORETICAL
682 DESCRIPTION OF HYDROGEL SWELLING: A REVIEW. *IRANIAN*
683 *POLYMER JOURNAL (ENGLISH), 19*(5 (119)), 375-398.

684 Garrec, D. A., & Norton, I. T. (2012). Understanding fluid gel formation
685 and properties. *Journal of Food Engineering, 112*(3), 175-182.
686 Garrec, D. A., & Norton, I. T. (2013). Kappa carrageenan fluid gel
687 material properties. Part 2: Tribology. *Food Hydrocolloids, 33*(1),
688 160-167.
689 Gholamipour-Shirazi, A., Norton, I. T., & Mills, T. (2019). Designing
690 hydrocolloid based food-ink formulations for extrusion 3D
691 printing. *Food Hydrocolloids, 95*, 161-167.
692 Gibaldi, M., & Feldman, S. (1967). Establishment of sink conditions in
693 dissolution rate determinations. Theoretical considerations and
694 application to nondisintegrating dosage forms. *Journal of*
695 *pharmaceutical sciences, 56*(10), 1238-1242.
696 Goyanes, Buanz, A. B., Basit, A. W., & Gaisford, S. (2014). Fused-
697 filament 3D printing (3DP) for fabrication of tablets.
698 *International journal of pharmaceutics, 476*(1-2), 88-92.
699 Goyanes, A., Scarpa, M., Kamlow, M., Gaisford, S., Basit, A. W., & Orlu,
700 M. (2017). Patient acceptability of 3D printed medicines. *Int J*
701 *Pharm, 530*(1-2), 71-78.
702 Grządka, E. (2015). Interactions between kappa-carrageenan and
703 some surfactants in the bulk solution and at the surface of
704 alumina. *Carbohydrate Polymers, 123*, 1-7.
705 Hansen, L. G., & Warwick, W. J. (1978). An improved assay method for
706 serum vitamins A and E using fluorometry. *American Journal of*
707 *Clinical Pathology, 70*(6), 922-923.
708 Hermansson, A.-M., Eriksson, E., & Jordansson, E. (1991). Effects of
709 potassium, sodium and calcium on the microstructure and
710 rheological behaviour of kappa-carrageenan gels. *Carbohydrate*
711 *Polymers, 16*(3), 297-320.
712 Hinton, T. J., Jallerat, Q., Palchesko, R. N., Park, J. H., Grodzicki, M. S.,
713 Shue, H.-J., Ramadan, M. H., Hudson, A. R., & Feinberg, A. W.
714 (2015). Three-dimensional printing of complex biological
715 structures by freeform reversible embedding of suspended
716 hydrogels. *Science advances, 1*(9), e1500758.
717 Iijima, M., Hatakeyama, T., & Hatakeyama, H. (2014). Gel–sol–gel
718 transition of kappa-carrageenan and methylcellulose binary

systems studied by differential scanning calorimetry. *Thermochimica Acta, 596*, 63-69.

Ito, A., & Sugihara, M. (1996). Development of oral dosage form for elderly patient: use of agar as base of rapidly disintegrating oral tablets. *Chemical and pharmaceutical bulletin, 44*(11), 2132-2136.

Jin, Y., Compaan, A., Bhattacharjee, T., & Huang, Y. (2016). Granular gel support-enabled extrusion of three-dimensional alginate and cellular structures. *Biofabrication, 8*(2), 025016.

Jones, D. S., Woolfson, A. D., & Brown, A. F. (1997). Textural, viscoelastic and mucoadhesive properties of pharmaceutical gels composed of cellulose polymers. *International journal of pharmaceutics, 151*(2), 223-233.

Jones, D. S., Woolfson, A. D., Djokic, J., & Coulter, W. (1996). Development and mechanical characterization of bioadhesive semi-solid, polymeric systems containing tetracycline for the treatment of periodontal diseases. *Pharmaceutical research, 13*(11), 1734-1738.

Kevadiya, B. D., Joshi, G. V., Patel, H. A., Ingole, P. G., Mody, H. M., & Bajaj, H. C. (2010). Montmorillonite-alginate nanocomposites as a drug delivery system: intercalation and in vitro release of vitamin B1 and vitamin B6. *Journal of biomaterials applications, 25*(2), 161-177.

Kim, H. W., Bae, H., & Park, H. J. (2017). Classification of the printability of selected food for 3D printing: Development of an assessment method using hydrocolloids as reference material. *Journal of Food Engineering, 215*, 23-32.

Kim, H. W., Lee, I. J., Park, S. M., Lee, J. H., Nguyen, M.-H., & Park, H. J. (2019). Effect of hydrocolloid addition on dimensional stability in post-processing of 3D printable cookie dough. *Lwt, 101*, 69-75.

Kim, H. W., Lee, J. H., Park, S. M., Lee, M. H., Lee, I. W., Doh, H. S., & Park, H. J. (2018). Effect of hydrocolloids on rheological properties and printability of vegetable inks for 3D food Printing. *Journal of food science, 83*(12), 2923-2932.

753 Koprnický, J., Najman, P., & Šafka, J. (2017). 3D printed bionic
754 prosthetic hands. In *2017 IEEE International Workshop of*
755 *Electronics, Control, Measurement, Signals and their Application*
756 *to Mechatronics (ECMSM)* (pp. 1-6).
757 Kouzani, A. Z., Adams, S., J. Whyte, D., Oliver, R., Hemsley, B., Palmer,
758 S., & Balandin, S. (2017). 3D Printing of Food for People with
759 Swallowing Difficulties. *KnE Engineering, 2*(2).
760 Kril, J. J. (1996). Neuropathology of thiamine deficiency disorders.
761 *Metabolic brain disease, 11*(1), 9-17.
762 Lanaro, M., Desselle, M. R., & Woodruff, M. A. (2019). 3D Printing
763 Chocolate. In *Fundamentals of 3D Food Printing and*
764 *Applications* (pp. 151-173).
765 Le Tohic, C., O'Sullivan, J. J., Drapala, K. P., Chartrin, V., Chan, T.,
766 Morrison, A. P., Kerry, J. P., & Kelly, A. L. (2018). Effect of 3D
767 printing on the structure and textural properties of processed
768 cheese. *Journal of Food Engineering, 220*, 56-64.
769 Li, H.-p., Li, H.-j., Qi, L.-h., Jun, L., & Zuo, H.-s. (2014). Simulation on
770 deposition and solidification processes of 7075 Al alloy droplets
771 in 3D printing technology. *Transactions of Nonferrous Metals*
772 *Society of China, 24*(6), 1836-1843.
773 Liang, S., Xu, J., Weng, L., Dai, H., Zhang, X., & Zhang, L. (2006). Protein
774 diffusion in agarose hydrogel in situ measured by improved
775 refractive index method. *Journal of controlled release, 115*(2),
776 189-196.
777 Lin, C. (2015). 3D Food Printing: A Taste of the Future. *14*(3), 86-87.
778 Liu, S., & Li, L. (2016). Thermoreversible gelation and scaling behavior
779 of Ca 2+ -induced κ-carrageenan hydrogels. *Food Hydrocolloids,*
780 *61*, 793-800.
781 Liu, Z., Zhang, M., & Yang, C.-h. (2018). Dual extrusion 3D printing of
782 mashed potatoes/strawberry juice gel. *Lwt, 96*, 589-596.
783 Long, J., Etxeberria, A. E., Nand, A. V., Bunt, C. R., Ray, S., & Seyfoddin,
784 A. (2019). A 3D printed chitosan-pectin hydrogel wound
785 dressing for lidocaine hydrochloride delivery. *Materials Science*
786 *and Engineering: C, 104*, 109873.

Lupo, B., Maestro, A., Gutiérrez, J. M., & González, C. (2015). Characterization of alginate beads with encapsulated cocoa extract to prepare functional food: comparison of two gelation mechanisms. *Food Hydrocolloids, 49*, 25-34.

McCue, T. (2012). 3D printing industry will reach $3.1 billion worldwide by 2016. *Retrieved, 3*(02), 2015.

Meena, R., Prasad, K., & Siddhanta, A. K. (2007). Effect of genipin, a naturally occurring crosslinker on the properties of kappa-carrageenan. *Int J Biol Macromol, 41*(1), 94-101.

Melocchi, A., Parietti, F., Loreti, G., Maroni, A., Gazzaniga, A., & Zema, L. (2015). 3D printing by fused deposition modeling (FDM) of a swellable/erodible capsular device for oral pulsatile release of drugs. *Journal of Drug Delivery Science and Technology, 30*, 360-367.

Nayak, K. K., & Gupta, P. (2015). In vitro biocompatibility study of keratin/agar scaffold for tissue engineering. *International journal of biological macromolecules, 81*, 1-10.

Ngo, T. D., Kashani, A., Imbalzano, G., Nguyen, K. T. Q., & Hui, D. (2018). Additive manufacturing (3D printing): A review of materials, methods, applications and challenges. *Composites Part B: Engineering, 143*, 172-196.

Nishinari, K. (1997). Rheological and DSC study of sol-gel transition in aqueous dispersions of industrially important polymers and colloids. *Colloid and Polymer Science, 275*(12), 1093.

Normand, V. (2003). Effect of sucrose on agarose gels mechanical behaviour. *Carbohydrate Polymers, 54*(1), 83-95.

Norton, I. T., Morris, E. R., & Rees, D. A. (1984). Lyotropic effects of simple anions on the conformation and interactions of kappa-carrageenan. *Carbohydrate research, 134*(1), 89-101.

Özcan, İ., Abacı, Ö., Uztan, A. H., Aksu, B., Boyacıoğlu, H., Güneri, T., & Özer, Ö. (2009). Enhanced topical delivery of terbinafine hydrochloride with chitosan hydrogels. *AAPS PharmSciTech, 10*(3), 1024.

Padzi, M., Bazin, M. M., & Muhamad, W. (2017). Fatigue Characteristics of 3D Printed Acrylonitrile Butadiene Styrene

(ABS). In *Materials Science and Engineering Conference Series* (Vol. 269, pp. 012060).
Patil, N. S., Dordick, J. S., & Rethwisch, D. G. (1996). Macroporous poly (sucrose acrylate) hydrogel for controlled release of macromolecules. *Biomaterials, 17*(24), 2343-2350.
Peppas, N. A., & Sahlin, J. J. (1989). A simple equation for the description of solute release. III. Coupling of diffusion and relaxation. *International journal of pharmaceutics, 57*(2), 169-172.
Pharmacopoeia, B. (2016). British pharmacopoeia.
Phillips, G. O., & Williams, P. A. (2000). *Handbook of hydrocolloids*: CRC press Boca Raton, FL.
Picker, K. M. (1999). Matrix tablets of carrageenans. II. Release behavior and effect of added cations. *Drug development and industrial pharmacy, 25*(3), 339-346.
Rahim, T. N. A. T., Abdullah, A. M., & Md Akil, H. (2019). Recent Developments in Fused Deposition Modeling-Based 3D Printing of Polymers and Their Composites. *Polymer Reviews, 59*(4), 589-624.
Rosas-Durazo, A., Hernández, J., Lizardi, J., Higuera-Ciapara, I., Goycoolea, F. M., & Argüelles-Monal, W. (2011). Gelation processes in the non-stoichiometric polylectrolyte–surfactant complex between κ-carrageenan and dodecyltrimethylammonium chloride in KCl. *Soft Matter, 7*(5), 2103-2112.
Rosenthal, A. J. (2010). Texture profile analysis–how important are the parameters? *Journal of Texture Studies, 41*(5), 672-684.
Rutz, A. L., Hyland, K. E., Jakus, A. E., Burghardt, W. R., & Shah, R. N. (2015). A multimaterial bioink method for 3D printing tunable, cell-compatible hydrogels. *Advanced Materials, 27*(9), 1607-1614.
Saha, D., & Bhattacharya, S. (2010). Hydrocolloids as thickening and gelling agents in food: a critical review. *J Food Sci Technol, 47*(6), 587-597.

Santoro, M., Marchetti, P., Rossi, F., Perale, G., Castiglione, F., Mele, A., & Masi, M. (2011). Smart Approach To Evaluate Drug Diffusivity in Injectable Agar−Carbomer Hydrogels for Drug Delivery. *The Journal of Physical Chemistry B, 115*(11), 2503-2510.

Serizawa, R., Shitara, M., Gong, J., Makino, M., Kabir, M. H., & Furukawa, H. (2014). *3D jet printer of edible gels for food creation* (Vol. 9058): SPIE.

Severini, C., Derossi, A., & Azzollini, D. (2016). Variables affecting the printability of foods: Preliminary tests on cereal-based products. *Innovative Food Science & Emerging Technologies, 38*, 281-291.

Severini, C., Derossi, A., Ricci, I., Caporizzi, R., & Fiore, A. (2018). Printing a blend of fruit and vegetables. New advances on critical variables and shelf life of 3D edible objects. *Journal of Food Engineering, 220*, 89-100.

Singh, B., Kaur, T., & Singh, S. (1997). Correction of raw dissolution data for loss of drug and volume during sampling. *Indian journal of pharmaceutical sciences, 59*(4), 196.

Singh, D., Singh, D., & Han, S. S. (2016). 3D Printing of Scaffold for Cells Delivery: Advances in Skin Tissue Engineering. *Polymers (Basel), 8*(1).

Sood, A. K., Ohdar, R. K., & Mahapatra, S. S. (2010). Parametric appraisal of mechanical property of fused deposition modelling processed parts. *Materials & design, 31*(1), 287-295.

Tako, M., & Nakamura, S. (1988). Gelation mechanism of agarose. *Carbohydrate research, 180*(2), 277-284.

Thrimawithana, T. R., Young, S., Dunstan, D. E., & Alany, R. G. (2010). Texture and rheological characterization of kappa and iota carrageenan in the presence of counter ions. *Carbohydrate Polymers, 82*(1), 69-77.

Tomšič, M., Prossnigg, F., & Glatter, O. (2008). A thermoreversible double gel: Characterization of a methylcellulose and κ-carrageenan mixed system in water by SAXS, DSC and rheology. *Journal of Colloid and Interface Science, 322*(1), 41-50.

Varghese, J. S., Chellappa, N., & Fathima, N. N. (2014). Gelatin–carrageenan hydrogels: role of pore size distribution on drug delivery process. *Colloids and Surfaces B: Biointerfaces, 113*, 346-351.

Ventola, C. L. (2014). Medical Applications for 3D Printing: Current and Projected Uses. *P & T : a peer-reviewed journal for formulary management, 39*(10), 704-711.

Vrentas, J., & Vrentas, C. M. (1992). Fickian diffusion in glassy polymer-solvent systems. *Journal of Polymer Science Part B: Polymer Physics, 30*(9), 1005-1011.

Wang, L., Zhang, M., Bhandari, B., & Yang, C. (2018). Investigation on fish surimi gel as promising food material for 3D printing. *Journal of Food Engineering, 220*, 101-108.

Warner, E. L., Norton, I. T., & Mills, T. B. (2019). Comparing the viscoelastic properties of gelatin and different concentrations of kappa-carrageenan mixtures for additive manufacturing applications. *Journal of Food Engineering, 246*, 58-66.

Watase, M., & Arakawa, K. (1968). Rheological properties of hydrogels of agar-agar. III. Stress relaxation of agarose gels. *Bulletin of the Chemical Society of Japan, 41*(8), 1830-1834.

Wei, J., Wang, J., Su, S., Wang, S., Qiu, J., Zhang, Z., Christopher, G., Ning, F., & Cong, W. (2015). 3D printing of an extremely tough hydrogel. *RSC Advances, 5*(99), 81324-81329.

Weiner, M. L. (1991). Toxicological properties of carrageenan. *Agents and actions, 32*(1-2), 46-51.

Wu, Y., Joseph, S., & Aluru, N. R. (2009). Effect of cross-linking on the diffusion of water, ions, and small molecules in hydrogels. *The Journal of Physical Chemistry B, 113*(11), 3512-3520.

Yang, F., Zhang, M., Bhandari, B., & Liu, Y. (2018). Investigation on lemon juice gel as food material for 3D printing and optimization of printing parameters. *Lwt, 87*, 67-76.

Yang, F., Zhang, M., Prakash, S., & Liu, Y. (2018). Physical properties of 3D printed baking dough as affected by different compositions. *Innovative Food Science & Emerging Technologies, 49*, 202-210.

924 Zhang, Y.-Q., Tsai, Y.-C., Monie, A., Hung, C.-F., & Wu, T.-C. (2010).
925 Carrageenan as an adjuvant to enhance peptide-based vaccine
926 potency. *Vaccine, 28*(32), 5212-5219.

927